G Protein-coupled pH-sensing Receptor OGR1 Is a Regulator of Intestinal Inflammation

de Vallière, Cheryl ; Wang, Yu ; Eloranta, Jyrki J ; Vidal, Solange ; Clay, Ieuan ; Spalinger, Marianne R ; Tcymbarevich, Irina ; Terhalle, Anne ; Ludwig, Marie-Gabrielle ; Suply, Thomas ; Fried, Michael ; Kullak-Ublick, Gerd A ; Frey-Wagner, Isabelle ; Scharl, Michael ; Seuwen, Klaus ; Wagner, Carsten A ; Rogler, Gerhard

Abstract: BACKGROUND A novel family of proton-sensing G protein-coupled receptors, including OGR1, GPR4, and TDAG8, was identified to be important for physiological pH homeostasis and inflammation. Thus, we determined the function of proton-sensing OGR1 in the intestinal mucosa. METHODS OGR1 expression in colonic tissues was investigated in controls and patients with IBD. Expression of OGR1 upon cell activation was studied in the Mono Mac 6 (MM6) cell line and primary human and murine monocytes by real-time PCR. Ogr1 knockout mice were crossbred with Il-10 deficient mice and studied for more than 200 days. Microarray profiling was performed using Ogr1 and Ogr1 (WT) residential peritoneal macrophages. RESULTS Patients with IBD expressed higher levels of OGR1 in the mucosa than non-IBD controls. Treatment of MM6 cells with TNF, led to significant upregulation of OGR1 expression, which could be reversed by the presence of NF- B inhibitors. Kaplan-Meier survival analysis showed a significantly delayed onset and progression of rectal prolapse in female Ogr1/Il-10 mice. These mice displayed significantly less rectal prolapses. Upregulation of gene expression, mediated by OGR1, in response to extracellular acidification in mouse macrophages was enriched for inflammation and immune response, actin cytoskeleton, and cell-adhesion gene pathways. CONCLUSIONS OGR1 expression is induced in cells of human macrophage lineage and primary human monocytes by TNF. NF- B inhibition reverses the induction of OGR1 expression by TNF. OGR1 deficiency protects from spontaneous inflammation in the Il-10 knockout model. Our data indicate a pathophysiological role for pH-sensing receptor OGR1 during the pathogenesis of mucosal inflammation.

DOI: https://doi.org/10.1097/MIB.0000000000000375

The G protein-coupled pH-sensing receptor OGR1 is a regulator of intestinal inflammation

Cheryl de Vallière[1*], Yu Wang[1,2*], Jyrki J. Eloranta[3] , Solange Vidal[4], Ieuan Clay[4], Marianne R. Spalinger[1], Irina Tcymbarevich[1], Anne Terhalle[1], Marie-Gabrielle Ludwig[4], Thomas Suply[4], Michael Fried[1], Gerd A. Kullak-Ublick[3], Isabelle Frey-Wagner[1], Michael Scharl[1], Klaus Seuwen[4], Carsten A. Wagner[2], Gerhard Rogler[1]

[1]Division of Gastroenterology and Hepatology, University Hospital Zürich, Switzerland, [2]Institute of Physiology, University of Zürich, Switzerland, [3]Department of Clinical Pharmacology and Toxicology, University Hospital Zürich, Switzerland, [4]Novartis Institutes for Biomedical Research, Basel, Switzerland

Corresponding author:

Gerhard Rogler, MD, PhD
Division of Gastroenterology and Hepatology
University Hospital Zürich
Rämistrasse 100
8091 Zürich
Switzerland
Tel. +41-(0)44-255-9477
E-mail: gerhard.rogler@usz.ch

* Cheryl de Vallière and Yu Wang contributed equally to this work.

ABSTRACT

Objective: A novel family of proton sensing G-protein coupled receptors (GPCRs), including *OGR1*, *GPR4*, and *TDAG8* was identified to be important for physiological pH homeostasis and inflammation. Thus we determined the function of proton-sensing OGR1 in the intestinal mucosa.

Design: *OGR1* expression in colonic tissues was investigated in controls and IBD patients. Expression of *OGR1* upon cell activation was studied in the Mono Mac 6 (MM6) cell line and primary human and murine monocytes by real-time PCR. *Ogr1* knockout mice were crossbred with *Il-10* deficient mice and studied over 200 days. Microarray profiling was performed using $Ogr1^{-/-}$ and $Ogr1^{+/+}$ (WT) residential peritoneal macrophages.

Results: IBD patients expressed higher levels of *OGR1* in the mucosa than non-IBD controls. Treatment of MM6 cells with TNF, led to significant up-regulation of *OGR1* expression, which could be reversed by the presence of NF-κB inhibitors. Kaplan-Meier survival analysis showed a significantly delayed onset and progression of rectal prolapse in female $Ogr1^{-/-}$// $Il\text{-}10^{-/-}$ mice. These mice displayed significantly less rectal prolapses. Up-regulation of gene expression, mediated by OGR1, in response to extracellular acidification in mouse macrophages was enriched for inflammation and immune response, actin cytoskeleton, and cell adhesion gene pathways.

Conclusion: *OGR1* expression is induced in cells of human macrophage lineage and primary human monocytes by TNF. NF-κB inhibition reverses the induction of *OGR1* expression by TNF. *OGR1* deficiency protects from spontaneous inflammation in the *Il-10* KO model. Our data indicate a pathophysiological role for pH-sensing receptor *OGR1* during the pathogenesis of mucosal inflammation.

Key Words: GPCR; pH-sensing receptors; *OGR1*; IBD; microarrays; animal model

Abbreviations: CD, Crohn's disease; DSS, dextran sulphate sodium; GAPDH, glyceraldehyde-3-phosphate dehydrogenase; GPCR, G protein coupled receptor; GPR4, G protein coupled receptor 4; GPR65, G protein coupled receptor 65; GPR68, G protein coupled receptor 68; H&E, hematoxylin and eosin; HPRT, Hypoxanthine-guanine phosphoribosyltransferase; IBD, inflammatory bowel disease; IFN-γ, interferon gamma; IL, interleukin; MPO, myeloperoxidase; OGR1, ovarian cancer G-protein coupled receptor 1; OR, odds ratio; PBS, phosphate buffered saline; RT-PCR, reverse transcription polymerase chain reaction; TDAG8, T-cell death associated gene 8; TNF, tumour necrosis factor; UC, Ulcerative colitis.

Grants: This work was supported by a collaborative grant from the Zürich Center for Integrative Human Physiology (ZIHP) to CW and GR, research grants from the Swiss National Science Foundation to GR (Grant No.314730-153380) and the Swiss IBD Cohort (Grant No 3347CO-108792). The funding institutions had no role in the study design, in the collection, analysis and interpretation of data and in the writing of the manuscript.

Competing interests: The authors declare no competing interests.

Author contributions: CdV performed experiments, analyzed the data and wrote the first draft of the manuscript; YW, SV, IC, MRS, IT, AT, M-GL, TS, performed experiments and were involved in data analysis, MF, GAK-U, IF-W, MS, JJE, KS, CAW, GR conceived, designed and supervised the study and respective experiments. All authors wrote, corrected and approved the manuscript.

INTRODUCTION

The mechanisms involved in the maintenance of mucosal homeostasis are important in our understanding of the pathophysiology of inflammatory bowel disease (IBD). Both forms of the disease, Crohn's disease (CD) and ulcerative colitis (UC), give rise to inflammation that is associated with extracellular acidification of mucosal tissue. Mucosal inflammation is interpreted as a local response to tissue damage and microbial invasion.

A number of studies suggest that an acidic environment affects the progression and resolution of inflammation.[1-3] Inflammation has been attributed to an increase in local proton concentration and lactate production[4] and subsequent pro-inflammatory cytokine production, such as tumour necrosis factor (TNF), interleukin-6 (IL-6), interferon-gamma (IFN-γ) and interleukin-1-beta (IL-1β). TNF is one of the characterizing cytokines in IBD[5, 6] and anti-TNF targeted therapies are successful in both CD and UC.[7-10] Activated macrophages, which are key cellular mediators of acute and chronic inflammation, are primary producers of TNF[11]. TNF activates the nuclear transcription factor kappa B (NF-κB), one of the key regulators in chronic mucosal inflammation.[12, 13]

G-protein-coupled receptors (GPCRs), cell-surface molecules involved in signal transduction, are targeted by key inflammatory cytokines.[14] The ovarian cancer G-protein coupled receptor 1 (*OGR1)* family of receptors, which include *OGR1*, G protein coupled receptor 4 *(GPR4)*, and T-cell death associated gene *(TDAG8)*, sense extracellular protons through histidine residues located on the extracellular region of the receptors, resulting in the modification of a variety of cell functions.[15, 16] Early signaling pathways of pH-sensing receptors triggered by acidification include phospholipase C activation, inositol trisphosphate formation and subsequent Ca^{2+} release[15] or cyclic adenosine monophosphate (cAMP) production.[17, 18] The increase of intracellular calcium influx and accumulation of cAMP has been shown to regulate a vast range of cellular responses. Moreover, *OGR1* and *TDAG8* are alleged to act in opposition in a regulatory manner, either enhancing or inhibiting the production of proinflammatory cytokines respectively.[19]

TDAG8 mediated extracellular acidification inhibited lipopolysaccharide (LPS)-induced production of TNF and IL-6 in mouse peritoneal inflammatory macrophages.[2] Patients with CD demonstrate a defect in macrophage function resulting in an inadequate bacterial clearance from inflammatory sites.[20] In addition, macrophages from CD patients showed impaired TNF-alpha secretion in response to bacterial challenge.[21] Furthermore,

association results and *in silico* analysis have recently identified a locus within the *TDAG8* gene as one of the susceptibility loci associated with CD.[22] Onozawa *et al*. suggest that *TDAG8* is a negative regulator of inflammation[23], which is mediated via a G_s-coupled mechanism.[2] In contrast, *OGR1* is reported to act predominately via a G_q-coupled mechanism to stimulate proinflammatory cytokines production upon extracellular acidification.[19]

To date, few data on the role of *OGR1* in inflammation in IBD have been published. *OGR1* may play an important role in the regulation of the inflammatory pathways in IBD, and it may represent an interesting target for innovative therapies. Therefore, we investigated the role and function of *OGR1* in gut inflammation, with a focus on myeloid cells. We used an immune-mediated inflammatory disease mouse model, namely interleukin-10 (*Il-10*) knockout (KO) mice, which spontaneously develop chronic colitis[24-26] and a human monocyte model. We show that *OGR1* expression is induced in monocytes by TNF and *Ogr1* deficiency protects from spontaneous inflammation in the *Il-10* KO model.

Materials and Methods

Details of reagents used and methods for gene expression are provided in the Supplementary Materials and Methods section.

pH experiments

pH shift experiments were carried out in serum-free RPMI medium (1-41F24-I, Amimed), supplemented with 2 mM Glutamax (35050-038, Gibco), and 20 mM HEPES. The pH of all solutions was adjusted using a calibrated pH meter (Metrohm, Herisau, Switzerland) with NaOH or HCl, and the medium was equilibrated in a 5% CO_2 incubator for 36 h. All data presented are referenced to pH measured at room temperature.

Culture of cell lines

The monocytic cell line MonoMac 6 (MM6, obtained from DMSZ) was cultured in RPMI (Sigma-Aldrich, Munich, Germany) supplemented with 10% FCS, 1% nonessential amino acids, and 1% oxalacetic acid–pyruvate–insulin medium supplement (Sigma-Aldrich), and maintained according to the American Type Culture Collection (ATCC).

Patient tissue samples

Primary intact colonic epithelial cell crypts were isolated from normal human colonic tissue of patients undergoing bowel surgery as previously described.[27] Biopsies of human terminal ileum, colon, or rectum were taken from patients with CD or UC, or from control subjects undergoing colonoscopy for colon cancer screening. Biopsies from patients with colitis were taken endoscopically from inflamed areas. Written consent was obtained before specimen collection and studies were approved by the local ethics committee.

Isolation of human peripheral blood monocytes

Normal human peripheral blood monocytes, obtained from the Swiss Red Cross Blood Service, were isolated from buffy coat samples, by density gradient centrifugation using Lymphoprep (Axis-Shield, Norway). Purification was performed using EasySep™ Human Monocyte Enrichment Kit without CD16 Depletion and EasySep magnet (both from Stemcell, Canada) according to manufacturer's instructions. The purity of the monocytes was > 85% as assessed by fluoroscein isothiocyanate (FITC)-labelled anti-CD14 (#557742, BD Biosciences, USA) by flow cytometry (data not shown).

Animal models

All animal experiments were performed according to Swiss animal welfare laws and were approved by the Veterinary Authority of Basel-Stadt and the Veterinary Office of the Canton Zürich, Switzerland. *Ogr*1$^{-/-}$ (C57BL/6) mice, initially obtained from Deltagen, Inc. - San Mateo, Ca, USA, were generated as described.[28] *Il-10* $^{-/-}$ mice (C57BL/6) mice and *Ogr*1$^{-/-}$ mice were crossed to generate *Ogr*1 $^{-/-}$ /*Il-10* $^{-/-}$ colitis susceptible mice. Mice were observed until reaching either 200 days of age or suffering a prolapse. All mice were housed together in one room in a vivarium.

Genomic DNA extraction and genotyping

Genotyping was confirmed by PCR of tail genomic DNA. DNA extraction was performed according to standard NaOH methods. The PCR reactions used for *Ogr1* genotyping were performed as previously described[28], oligonucleotides used are listed in the supplementary material and methods.

Murine macrophage isolation and culture

Mature quiescent macrophages were isolated from the mouse peritoneal cavity without the aid of eliciting agents, as described by Zhang *et al.*[29] Animals were sacrificed by cervical dislocation to reduce influence on pH. Further details are described in the supplementary methods.

Evaluation of inflammation in murine colitis

Typical inflammatory parameters were evaluated as previously described.[30, 31]

Expression Profiling by Microarrays

Global whole-transcript analysis was performed using a GeneAtlas microarray system (Affymetrix) to compare response differences between *Ogr*1$^{+/+}$ and *Ogr*1$^{-/-}$ murine macrophages after 24 h acidic pH shift. Mature murine quiescent peritoneal macrophages were isolated as described above, from age matched female *Ogr*1 $^{-/-}$ and *Ogr*1 $^{+/+}$ mice (C57BL/6). Five replicates or mice per condition were used, and ≈ 1 x 10^6 macrophages/per mouse obtained. Cells were not pooled. Cells were treated with pH 6.7 equilibrated medium to activate *Ogr1,* and pH 7.7 to serve as negative controls. Cells were collected, and RNA and cDNA samples prepared. Biotin-labelled cDNA samples were hybridized to GeneChip Mouse Gene 1.1ST Array Strip (Affymetrix, P/N 901628) following protocols provided by Affymetrix. Data was summarized on gene-level using RMA (Robust Multi-array Average). Data quality was assessed using the bioconductor/R package 'arrayQualityMetrics'[32] and reproducibility was assessed using Pearson's correlation for all the filtered expression values and hierarchical clustering. For all pairwise comparisons, differentially expressed genes were selected using ≥2.0-fold-change, $P<0.05$ significance, as determined using ANOVA (as implemented by the R package, Linear Models for Microarray Data, 'limma') and F-test for the complete experimental design. The results were analyzed by global ranked fold change and using Metacore software for pathway enrichment.

Statistical Analysis

For murine prolapse ratio comparison studies, statistical differences between genotypes were calculated by chi-square test with Fisher's exact test (exact significance, two sided) and risk estimate test from contingency tables. The prolapse survival analysis was

performed using Kaplan-Meier survival analysis (log rank Mantel-Cox test) and estimated median survival time. Groups of data were compared using nonparametric Mann-Whitney U-test (mouse data) or Kruskal-Wallis one-way ANOVA followed by Dunn's multiple-comparison test (patient data). Data are presented as mean ± SEM for a series of n experiments. Probabilities (p, two tailed) of $p < 0.05$ were considered statistically significant. Monocyte/macrophage expression data were analyzed using a one-way analysis of variance (ANOVA) followed by the Tukey Post Hoc test. Throughout this manuscript, asterisks denote significant differences at *=p<0.05, **=p<0.01, ***=p<0.001.

RESULTS

OGR1 mRNA expression is increased in IBD patients

OGR1 mRNA expression in isolated crypts and terminal ileum, colon, or rectum specimens from IBD patients and control subjects was confirmed by RT-qPCR. Ct values from the isolated crypts from 4 patients ranged from 27 to 30, indicating moderate expression of *OGR1* in colonic epithelium (data not shown). Compared with normal control subjects, *OGR1* expression increased 2.3 -fold (p<0.05) in UC patients (n=8) and 2.2 -fold (p<0.01) in CD patients (n=29) (Figure 1).

OGR1 expression is regulated by TNF in myeloid cells

A local decrease in pH usually occurs at inflammatory sites, and monocytes are rapidly recruited, followed by an increase in pro-inflammatory cytokines. MM6 cells were treated with IFN-γ, IL-1β, IL-6, TNF or TGF-β, which are known to initiate immune and inflammatory responses in the mucosa. Stimulation by TNF resulted in significant up-regulation of *OGR1* expression (≈4-5-fold p<0.001, Figure 2A-B). No induction of *OGR1* occurred by IFN-γ, IL-1β, IL-6 or TGF-β at 6 h (Figure 2A-B) or at 1 h, 5 h or 24 h (data not shown). A concentration-dependent (0, 2.5, 10, 25, 50, 100 ng/ml) induction of *OGR1* mRNA expression in MM6 cells by TNF was confirmed at 4 and 8 h (Figure 2C). Maximal OGR1 induction, after 8 h treatment was reached at TNF concentration 50 ng/ml (Figure 2C). Induction of *OGR1* expression in MM6 cells by TNF returned to basal levels after 48 h (Figure 2D).

Treatment of MM6 cells with PMA, a known PKC activator but also commonly used to differentiate monocytes into macrophage-like cells[33], led to increased *OGR1* expression (14 -fold at 24 h, p< 0.001) (Figure 2E).

To confirm the relevance of our findings in MM6 cells, we tested OGR1 -induction by TNF and PMA in primary human monocytes and mouse peritoneal macrophages. Concentration-dependent TNF and PMA induction of *OGR1* mRNA was confirmed in human monocytes (Figure 3A-B). Similarly TNF -mediated OGR1 induction was observed in mouse macrophages (Figure 4). The intensity of the response to TNF was comparable in MM6 cells and primary mouse macrophages (Figure 2C-D MM6; Figure 4). The induction time of primary human monocytes was considerably slower but of similar intensity. Similarly, primary human monocytes exhibited a slower induction and lower response to PMA compared to MM6 cells. No induction of the other pH-sensing GPCRs *GPR4* and *TDAG8*, by any of the cytokines tested or by PMA was detected (data not shown).

TNF, LPS or PMA induced *OGR1* expression is reversed by Akt, MAP and PKC kinase and NF-κB inhibitors

To understand the pathways involved in TNF, PMA or LPS-mediated induction of *OGR1* expression we investigated the roles of Akt1/2 kinase, c-Jun N-terminal kinase (JNK) and PKC by using their specific inhibitors. Mitogen-activated protein kinases (MAPKs) play an important role in regulating the cellular response to various extracellular stimuli.[34] Signaling via PKC is known to activate MAPKs.[35] Activation occurs by sequential phosphorylation by JNK, ERK (extracellular-signal-regulated kinase) 1/2, p38 MAPK, ERK5 and ERK3/4.[36] Activated MAPK kinase pathways may stimulate activator protein 1 (AP-1).[37,38] Exposure of monocytes and macrophages to TNF, LPS and PMA results in activation of the AP-1, NF-κB, caspase and MAPK pathways.[39, 40] Akt is a serine-threonine kinase and has been implicated in TNF-mediated activation of NF-κB.[41, 42]

Based on our time course experiments (Figure 2D), cells were stimulated with PMA, TNF or LPS, in the presence of the appropriate kinase inhibitor, A6730 (9 μM), SP600125 (20 μM) and curcumin (25 μM), and harvested after 6 hours.

Exposure of MM6 cells to PMA, TNF and LPS induced *OGR1* expression 13.7, 8.2 and 10.3 -fold respectively. The Akt1/2 kinase inhibitor, A6730, significantly decreased TNF and LPS -induced *OGR1* expression, by 5.6 (68%) and 8.2 -fold (80%) respectively, but with less effect on PMA activation (4.8 -fold decrease, 35% decrease) (n=2, $p<0.001$ or 0.01, Figure 5A). SP600125, a JNK inhibitor, decreased *OGR1* induction by PMA 10.1 -fold, (73%) TNF 4.0 -fold (48%) and LPS 7.5 -fold (80%). These results suggest that the JNK/AP1 pathway may be involved in *OGR1* regulation. Curcumin is a potent inhibitor of

protein kinase C[43] and inhibits NF-κB activation through inhibition of IκB kinase and Akt activation.[44] Curcumin abolished the induction of all three activating agents (PMA 12.7 -fold (93%), TNF 7.2 -fold 87% and LPS 9.9 -fold 96% decrease). These preliminary kinase inhibitor studies suggest that Akt1/2, JNK, PKC and IKK pathways play an important role in the induction of *OGR1* expression by PMA, TNF and LPS.

Prompted by the results we next tested a number of known NF-κB inhibitors. TNF-, PMA-, or LPS-mediated induction of *OGR1* was significantly reduced by simultaneous treatment of cells with NF-κB inhibitors: curcumin (25 μM), MG-132 (20 μM), AICAR (0.5 nM), BAY-11-7082 (20 μM), CAY10512 (0.3 μM), and SC-514 (25 μM) (Figure 5A-C). In the presence of the inhibitor MG132, TNF induced *OGR1* expression decreased 3.2 and 5.7 -fold respectively (TNF 95% decrease, PMA 89% decrease) (n=2, $p< 0.001$, Figure 5B).

AICAR (5-Aminoimidazole-4-carboxyamide) ribonucleoside blocks the expression of pro-inflammatory cytokines genes by a reduction in NF-κB DNA-binding activity[45]. BAY-11-7082 and SC-514 block NF-kB activation by inhibition of IκB kinase.[46, 47] The resveratrol analog CAY10512 is a specific NF-κB inhibitor. Treatment with PMA, TNF or LPS resulted in 10.2, 3.0 or 7.6 -fold increase in *OGR1* expression respectively, but in the presence of the NF-κB inhibitors induction of *OGR1* significantly decreased. *OGR1* expression decreased with inhibitor; AICAR 9.3-, 2.6- and 7.3 -fold / (91%, 88%, 96%) ; BAY 7082, 9.0-, 2.6- and 6.1 -fold / (88%, 87%, 81%); Cay 10512, 5.6-, 1.8- and 3.8 -fold / (56%, 62%, 49%), ; SC-514, 8.7-, 2.7- and 7.4 -fold (85%, 91%, 97%) on PMA, TNF and LPS stimulation, respectively (Figure 5C). The results collectively suggest that NF-κB plays a key role in the regulation of *OGR1*.

In silico analysis of the *OGR1* promoter

As the inhibitor studies suggested a strong role for AP-1[48] and NF-κB in the regulation of *OGR1* expression we next performed an *in silico* promoter analysis of *OGR1*. Two alternative predicted promoter variants ≈ 9 kpb apart, exist for the *OGR1* gene on chromosome 14. *In silico* analysis using MatInspector software[49] (http://www.genomatix.de/matinspector.html) revealed several putative DNA-binding sites for AP-1, NF-κB and HIF-1α within the proximal regions of the *OGR1* promoter variants. A schematic representation of these sites (TBSs) for *OGR1* variants 1 and 2 and binding sites are shown in Supplemental Figure S1 and S2, respectively.

Cellular responses upon *OGR1* activation by extracellular acidification in murine macrophages.

We further investigated the effect of OGR1 deficiency on intestinal inflammation. We conducted a microarray study and compared the global gene expression of wild type *Ogr1*$^{+/+}$ cells to *Ogr1*$^{-/-}$ cells in response to extracellular acidification. We selected the top 100 most differentially expressed genes by comparing the ranked fold change upon pH shift in WT compared to KO macrophages. Figure 6A shows a heat map summarizing gene expression across all samples in the 4 experimental conditions for these 100 genes.

Acid-induced *OGR1*-mediated differentially up-regulated genes in WT macrophages compared to *OGR1* KO macrophages include inflammatory response genes (*Tnfrsf13c, Ccl24, Cxcl13, C1qa, Nr4a1)* and immune response genes (*Iglv1, Cd79a, H2-Eb1, Tinagl1, Lst1, C1qa, C1qb Cd83, Ccl17*). Furthermore, genes associated with adhesion and ECM (*Sparc, Cyr61, Timp1, Aebp1, Ebp1, Siglec1, Cdh2, Mmp11, Serpine2, Tgm2*), and actin cytoskeleton (*Inhba, Fscn1, Sorbs2, Tuba1c, Map1b, Parva, Cnn3*) were up-regulated by acidic activation of *OGR1* in WT but not in *OGR1* KO macrophages. Interestingly, cholesterol homeostasis genes, (*Cyp11a1, Ephx2*), glucose response and insulin processing genes, (*Inhba, Cpe, Cma1, Igfbp7, Htra1, Sfrp4*), differentiation and bone development gene *Bmp-2* and transcription factor gene *Nrbf2* also increased in WT *Ogr1*$^{+/+}$ compared to *Ogr1*$^{-/-}$ KO cells at acidic pH.

The scatter plot represents the ratio fold change low to high pH *OGR1* KO /fold change low to high pH WT macrophages (Figure 6B). The top 100 differentially expressed genes are shown in Supplementary Tables S2.A–B. In addition, a list of genes and enrichment pathways, generated in GeneGo by comparison of pairs of WT low pH vs. high pH to OGR1 KO low pH vs. high pH, is shown in supplementary Table S3 and Figure S3 respectively. Results discussed in this paper have been deposited in the NCBI Gene Expression Omnibus (GEO) Accession No. GSE60295 (http://www.ncbi.nlm.nih.gov/projects/geo).

OGR1 deficiency protects from development of spontaneous colitis in mice

To investigate whether the *OGR1* dependent changes upon acidification have functional consequences during IBD, we applied a mouse model of spontaneous colitis. Analysis of the occurrence of prolapse in the colon over the course of 200 days showed that, only 16.7% of female *Ogr1*$^{-/-}$/*Il-10*$^{-/-}$ mice (n=24) developed rectal prolapse. The incidence was

significantly lower than that of female *Ogr1*$^{+/+}$/*Il-10*$^{-/-}$ littermate *mice* (66.7%, n=12) maintained in the same vivarium room during the same time period (p = 0.007**; Odds Ratio for female mice *Ogr1* $^{-/-}$/*Ogr1*$^{+/+}$ = 0.100 (95% CL 0.020∼0.500), chi-square test with Fisher's exact test with two sides). Kaplan-Meier survival analysis showed a significantly delayed onset and progression of rectal prolapse in female *Ogr1*$^{-/-}$/*Il-10*$^{-/-}$ mice (estimated median survival time: >200 days vs. 123 days for female *Ogr1*$^{+/+}$/*Il-10*$^{-/-}$ mice, p=0.002 **, log rank (Mantel-Cox) test) (Figure 7). No prolapses were observed in control *Ogr1*$^{+/+}$/*Il-10*$^{+/+}$ mice (n > 100 animals).

Histologically, consistent with the prolapse ratios, *Ogr1*$^{-/-}$/*Il-10*$^{-/-}$ mice showed less inflammation (score 3.7±1.03) (Figure 8A), however, this difference did not reach statistical significance from *Ogr1*$^{+/+}$/*ll-10* $^{-/-}$ female mice (6.5±1.12) (p>0.05, Figure 8B). The same trend in MPO levels of female *Ogr1* $^{-/-}$/*Il10*$^{-/-}$ mice was observed (0.12±0.034 vs. 0.41±0.072, p>0.05, Figure 9A). There were no differences in colon length, relative spleen weight (Figure 9B-C) and in cytokines mRNA expression levels (Figure 10).

Discussion

Our manuscript provides evidence for a role of the pH-sensing receptor *OGR1*, in inflammatory processes such as intestinal inflammation. We show that *OGR1* mRNA expression is up-regulated ≈ 2 -fold during intestinal inflammation in IBD patients. To what extent this translates into up-regulated protein expression cannot currently be assessed due to a lack of suitable antibodies. We further show that the pro-inflammatory cytokine TNF, a major mediator in IBD associated inflammation induces *OGR1* expression in human and murine myeloid cells. TNF up-regulates *OGR1* expression for short periods (6 to 12 h), however, the effect is not sustained for longer periods, after 24 - 48 h *OGR1* expression returns to basal levels.

Similar to our findings, Lum and coworkers reported that expression of *GPR4*, a related proton sensing GPCR, is up-regulated several-fold by TNF and H_2O_2 in human brain microvascular endothelial cells.[50] TNF-mediated induction of *GPR4* occurred after 2 h and was sustained for 24 h.[50] However, in contrast to OGR1, we did not observe induction of *GPR4* and *TDAG8* expression upon treatment with TNF, PMA, or LPS in MM6 cells. *OGR1* expression induced by TNF, PMA or LPS was prevented by treatment with PI-3 (Akt1/2), MAP and PKC inhibitors and with NF-κB inhibitors AICAR, BAY-11-7082, CAY10512, and SC-514. LPS stimulates production of TNF in MM6 cells.[51, 52]

We further show that genetic deletion of *OGR1* ameliorates inflammation at least in female mice. Acidification and signaling via *OGR1* induced a multitude of cellular responses in the microarray analysis. In murine macrophages acid induced *OGR1*-mediated enriched up-regulated genes are involved in inflammatory responses, further supporting our finding that *OGR1* signaling upon pH changes may play an important role in mucosal inflammation. Notably, up-regulation of nuclear receptor subfamily 4 group A member 1 (NR4A1, also known as NUR77) was detected (Supplementary Table S3). NR4A1 functions as an immediate early-response gene and plays a key role in mediating inflammatory responses in macrophages.[53] Further affected pathways are actin cytoskeleton modulation and cell adhesion. This may also be relevant as anti-adhesion strategies for the treatment of IBD have been recently successful and vedolizumab as an antibody against α4β7 integrin recently has been approved for therapy of Crohn's disease by the FDA and EMA. In an *OGR1*-overexpressing Caco2 model we also observed enrichment of inflammatory response, including NR4A1, actin cytoskeleton, and adhesion and ECM genes upon acidification (manuscript in submission). In the present study, the genes Inhba and Nr4a1 which are linked to the myocardin-related transcription factor (MRTF) pathway[54], were also found to be strongly regulated by pH change.

Another strongly regulated gene was activin. Activin A is released early in the cascade of circulatory cytokines during systemic inflammatory episodes, roughly coincident with TNF and before IL-6 and follistatin are elicited. Activin A protein is also elevated in IBD patients and in experimental colitis.[55] Recently activin A was identified to regulate macrophage switch between polarization states.[56] This skew towards a pro-inflammatory phenotype occurs by promoting the expression of M1 (GM-CSF) markers, and impairing the acquisition of M2 (M-CSF) markers, while down-regulating the production of *Il-10*.[56] Furthermore, *SPARC* (Secreted protein acidic and rich in cysteine) was found to be strongly regulated by *OGR1*. *SPARC* is a gene whose methylation has been related to IBD.[57, 58] *SPARC* exacerbates colonic inflammatory symptoms in DSS-induced murine colitis. Compared to WT, *SPARC* KO mice had less inflammation with fewer inflammatory cells and more regulatory T cells.[59]

Why would pH-sensing be so important during intestinal inflammation? Firstly, pH homeostasis is important for the maintenance of normal cell function. pH is normally tightly controlled within a narrow range. Normal pH of blood and tissue is controlled at ≈ pH 7.2- 7.4. Maintaining homeostasis requires cells to sense their external environment,

communicate with each other, and respond rapidly to extracellular signals. This can be achieved by hydrophobic molecules, ion channels, catalytic receptor and G-protein-coupled receptors.[60]

Under physiological conditions there are also counterplayers of *OGR1* expressed in the mucosal tissue. *TDAG8* mediates extracellular proton-induced inhibition of proinflammatory cytokine production in mouse macrophages.[2] Onozawa *et al.* showed that *TDAG8* deficient mice exhibit enhanced arthritic symptoms compared to wild type animals; suggesting that *TDAG8* attenuates inflammation by negatively regulating the function of the macrophages, T cells and B cells.[23] In search for genetic components and causal genetic variants of IBD, genome-wide association (GWA) studies have identified numerous susceptibility regions that are marked by single nucleotide polymorphisms (SNPs).[22, 61, 62] Association results and *in silico* analysis identified a locus within the *TDAG8* gene as susceptibility locus in CD[22], supporting that *TDAG8* acts as a negative regulator of inflammation. Khor *et al.* propose that the presence of *TDAG8* as an IBD-risk loci is necessary to maintain intestinal homeostasis due to its immune modulatory effect.[63]

To summarize, ORG1 expression is induced in human and murine myeloid cells by TNF, PMA and LPS; whereby simultaneous treatment with NF-κB inhibitors caused a reversal of this effect. Up-regulated genes induced by extracellular low pH by proton-sensing OGR1 IN murine macrophages were enriched for inflammatory and immune response, actin cytoskeleton and cell adhesion genes sets. The deficiency of pH-sensing receptor *OGR1* protects from spontaneous inflammation in the *Il-10* KO model. Thus, pH sensors may be interesting new targets for pharmacological intervention in intestinal inflammation.

Acknowledgements

We thank Jelena Kühn Georgijevic, Lennart Opitz, Michal Okoniewski and Hubert Rehrauer from the Functional Genomics Center Zürich for the microarray service/analysis and Andreas Sailer and Miroslava Vanek for providing human monocytes. Agnes Feige, Alexandra Cee, Christian Hiller and Silvia Lang are acknowledged for their expert technical assistance. The help from the ZIRP Rodent Phenotyping Facility is gratefully acknowledged.

FIGURE AND TABLE LEGENDS

Figure 1. OGR1 expression in human intestinal mucosa

IBD patients expressed higher levels of *OGR1* mRNA in the mucosa as compared to controls. Expression levels normalized to GAPDH. Biopsy specimens were taken from 29 CD patients, 8 UC patients and 17 non-IBD control patients. Asterisks denote significant differences from the respective control (*P < 0.05, **P < 0.01, ***P <0 .001).

Figure 2. TNF and PMA induce *OGR1* expression in human monocytes

A – B. MonoMac6 (MM6) cells were treated with cytokines for 6 hours. Treatment of MM6 cells with TNF led to significant up-regulation of *OGR1.* No induction of *OGR1* occurred with other cytokines (IFN-γ, IL-1β, IL-6, TGF-β) (50 ng/ml) tested. **C.** Concentration-dependent TNF (0, 2.5, 10, 25, 50, 100 ng/ml) induction of *OGR1* mRNA expression was confirmed at 4 and 8 h. Maximal *OGR*1 induction was reached at TNF concentration 50 ng/ml at 8 h. **D.** Induction of *OGR1* expression by TNF (50 ng/ml) returned to basal levels after 48 h. **E.** Monocytic-macrophagic differentiation of MM6 cells with phorbol 12-myristate 13-acetate (PMA) (25 nM), a specific activator of protein kinase C (PKC) and NF-κB, led to a significant increase in *OGR1* mRNA expression**.** Asterisks denote significant differences from the respective control (*P < 0.05, **P < 0.01, ***P <0 .001). Representative data of one of three qualitatively similar experiments shown unless indicated.

Figure 3. TNF- and PMA-dependent induction of *OGR1* mRNA in primary human monocytes. A. Dose-dependence of TNF (0, 2.5, 10, 25, 50 ng/ml) induction of *OGR1* mRNA was confirmed in primary human monocytes. **B.** PMA (0, 5, 25, 50, 75, 100 ng/ml) induction of *OGR1* mRNA was confirmed in primary human monocytes. Asterisks denote significant differences from the respective control (*P < 0.05, **P < 0.01, ***P <0 .001). Representative data of one of two similar experiments shown.

Figure 4. TNF induces *OGR1* expression in murine macrophages. *OGR1* induction by TNF (25 ng/ml) was also confirmed in primary mouse residential peritoneal macrophages. Asterisks denote significant differences from the respective control (*P < 0.05, **P < 0.01, ***P <0 .001). Representative data of one of three similar experiments shown.

Figure 5._TNF-, PMA-, and LPS-mediated induction of *OGR1* in MM6 cells was reversed by simultaneous treatment of cells with kinase and NF-kB inhibitors. A. Kinase inhibitors, A6730 (9 μM), SP600125 (20 μM) and curcumin (25 μM), reduced or abolished TNF (25 ng/ml), PMA (25 nM), or LPS (1 μg/ml) mediated induction of *OGR1* in MM6 cells. **B.** Treatment with NF-kB inhibitor MG-132 (20 μM) significantly reduced TNF (50 ng/ml) or PMA (25 nM) mediated induction of *OGR1* in MM6 cells. **C.** AICAR (0.5 nM), BAY-11-7082 (20 μM), CAY10512 (0.3 μM), and SC-514 (25 μM) also reduced TNF (25 ng/ml), PMA (25 nM), or LPS (1 μg/ml) mediated induction of *OGR1.* Asterisks denote significant differences from the respective control (*P < 0.05, **P < 0.01, ***P <0 .001). Representative data of one of two similar experiments shown.

Figure 6. Global gene expression of acid response of mouse macrophages. A. Top 100 genes from the whole-transcript microarray analysis of acid response (pH 6.7) of wild type (WT) and Ogr1 KO murine macrophages**.** Control condition, pH 7.7 is shown on the left. Changes in gene expression within each comparison are represented as Log2-transformed fold changes (≥2.0-absolute-fold-change, P<0.05 significance). **B.** Differentially expressed genes for acid response in WT and *OGR1* KO macrophages. Fold changes in low to high pH shift of *OGR1* KO macrophages are depicted on y-axis and fold changes low to high pH WT macrophages are shown on the x-axis. The highest ranking differentially expressed genes in the acid response of WT mouse macrophages are shown in the lower right quadrant of the scatter plot and the upper left quadrant shows the highest ranking differentially expressed genes in the acid response of *OGR1* KO mouse macrophages.

Figure 7. *OGR1* deficient mice show delayed onset and severity of prolapse in a spontaneous *IL-10* knock out mouse model. Kaplan-Meier survival analysis showed a significantly delayed onset and progression of rectal prolapse in female *Ogr1* $^{-/-}$*/Il-10* $^{-/-}$ *mice* (estimated median survival time: >200 days vs. 123 days, p=0.002 **, log rank (Mantel-Cox) test). Green solid lines, *Ogr1* $^{-/-}$*/Il-10* $^{-/-}$ mice (16.7% prolapses, n=24); blue solid line, *Ogr1* $^{+/+}$*/Il-10* $^{-/-}$ mice (66.7% prolapses, n=12); grey solid lines, *Ogr1*$^{+/+}$*/Il-10*$^{+/+}$ mice (0% prolapses, n=31). No rectal prolapses were detected in any of the *Ogr1*$^{+/+}$*/Il-10*$^{+/+}$ mice in the breeding colony in the study, 200 days.

Figure 8. *OGR1* deficient mice exhibit a trend to less inflammation in a spontaneous *IL-10* knock out mouse model A. Microscopic analysis of terminal colon sections from *Ogr1* $^{-/-}$*/Il-10* $^{-/-}$, *Ogr1*$^{+/+}$*/Il-10*$^{-/-}$ and *Ogr1*$^{+/+}$*/Il-10*$^{+/+}$ 80-day-old mice, staining by

Hematoxylin and eosin. Representative images are shown. **B.** Histological score, based on evaluation of morphological changes of epithelium and immune cell infiltration, of distal colon from *Ogr1* $^{-/-}$*/Il-10* $^{-/-}$, *Ogr1*$^{+/+}$*/Il-10* $^{-/-}$ and *Ogr1*$^{+/+}$*/Il-10*$^{+/+}$ 80-day-old mice. Data presented as mean ± SEM; n ≥ 5 per group; Asterisks denote significant differences from the respective control (*P < 0.05, **P < 0.01, ***P <0 .001). All mice were female.

Figure 9. The development of IBD and progression of prolapse between *Ogr1* $^{-/-}$*/IL-10* $^{-/-}$ and *Ogr1*$^{+/+}$*/Il-10*$^{-/-}$ *female* mice. **A.** Comparison of MPO activity in colon tissue **B.** Assessment of colon length. **C.** Relative spleen weight. No significant differences in OGR1 KO/Il-10 KO mice and controls in these parameters were observed.

Figure 10. Expression levels of cytokines in colons of female *Ogr1* $^{-/-}$*/Il-10* $^{-/-}$*, Ogr1* $^{+/+}$*/Il-10* $^{-/-}$ and *Ogr1* $^{+/+}$*/Il-10*$^{+/+}$ (WT control) mice were determined by real-time PCR and normalized to GAPDH. (n= 6∼9 mice per group). The homogenate of each mouse colon sample was tested in triplicate. Data presented as mean ± SEM; Asterisks denote significant differences from the respective control (*P < 0.05, **P < 0.01, ***P <0 .001). No statistical difference between colon and mesenteric lymph nodes of female *Ogr1* $^{-/-}$*/Il-10*$^{-/-}$ mice and female *Ogr1* $^{+/+}$*/Il-10* $^{-/-}$ mice was observed (p>0.05, Kruskal-Wallis one-way ANOVA followed by Dunn's multiple-comparison test).

Figures.

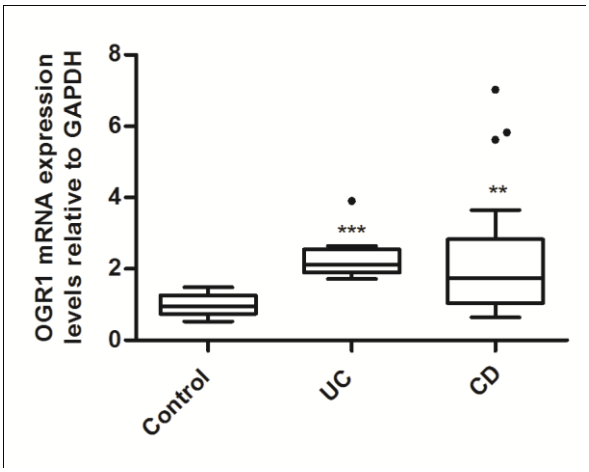

Figure 1.

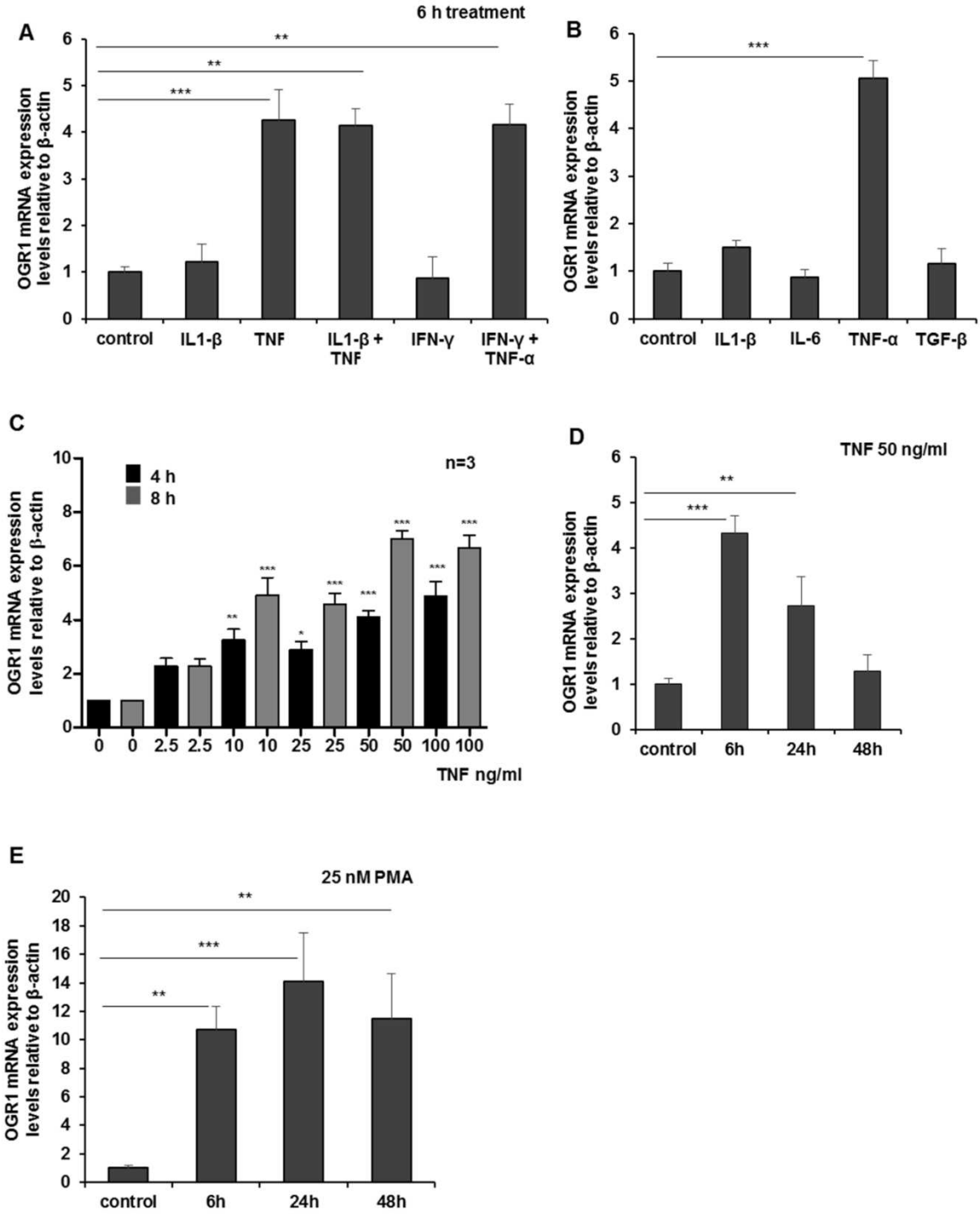
A
6 h treatment
OGR1 mRNA expression levels relative to β-actin
control
IL1-β
TNF
IL1-β + TNF
IFN-γ
IFN-γ + TNF-α
B
OGR1 mRNA expression levels relative to β-actin
control
IL1-β
IL-6
TNF-α
TGF-β
C
4 h
8 h
n=3
OGR1 mRNA expression levels relative to β-actin
0 0 2.5 2.5 10 10 25 25 50 50 100 100
TNF ng/ml
D
TNF 50 ng/ml
OGR1 mRNA expression levels relative to β-actin
control
6h
24h
48h
E
25 nM PMA
OGR1 mRNA expression levels relative to β-actin
control
6h
24h
48h

Figure 2.

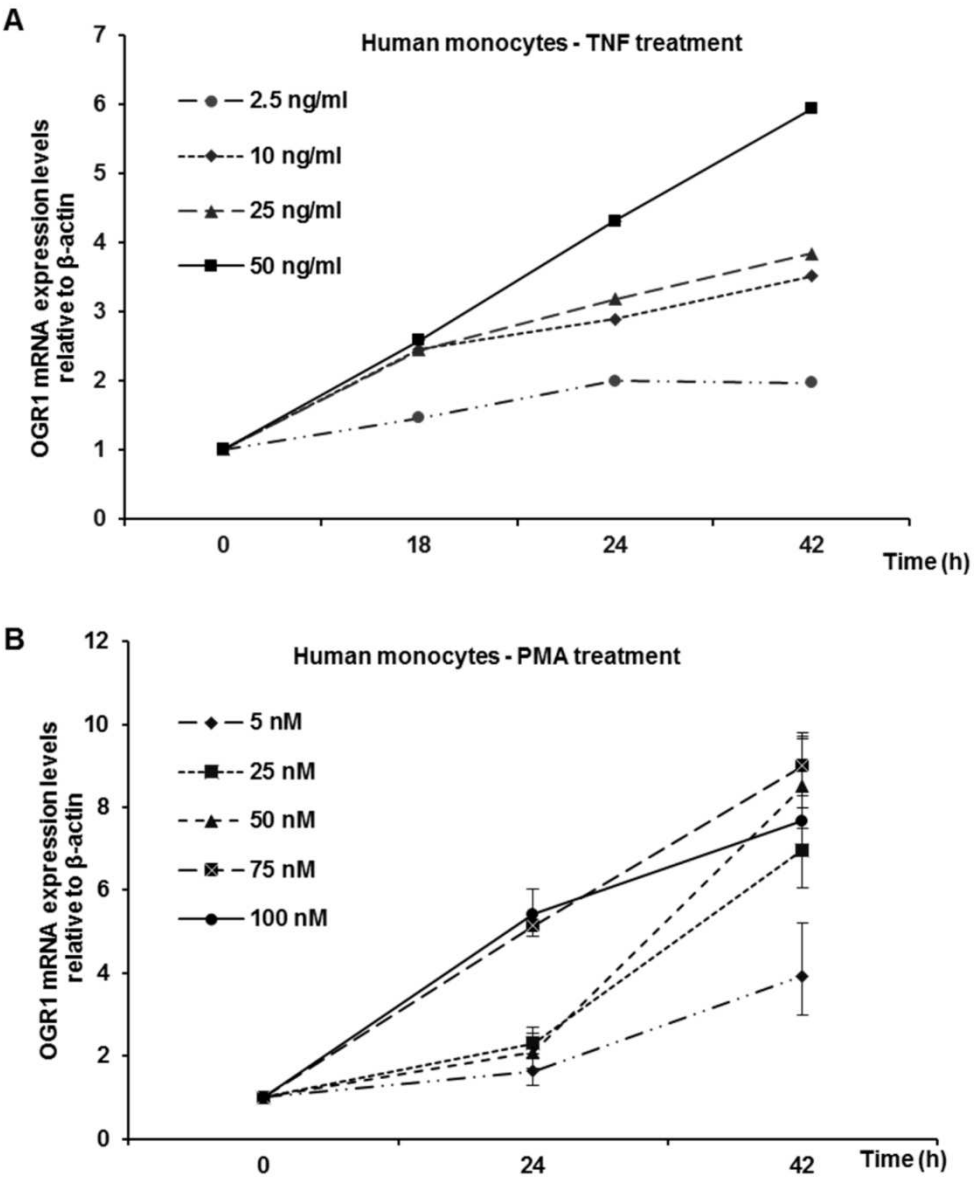
A
Human monocytes - TNF treatment
2.5 ng/ml
10 ng/ml
25 ng/ml
50 ng/ml
OGR1 mRNA expression levels relative to β-actin
0
1
2
3
4
5
6
7
0
18
24
42
Time (h)
B
Human monocytes - PMA treatment
5 nM
25 nM
50 nM
75 nM
100 nM
OGR1 mRNA expression levels relative to β-actin
0
2
4
6
8
10
12
0
24
42
Time (h)

Figure 3.

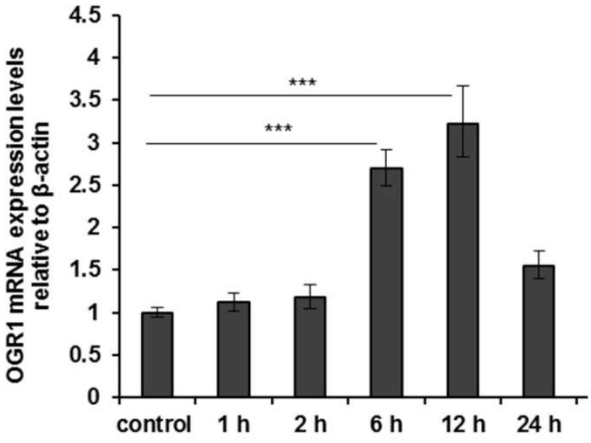
OGR1 mRNA expression levels relative to β-actin
4.5
4
3.5
3
2.5
2
1.5
1
0.5
0
***
***
control
1 h
2 h
6 h
12 h
24 h

Figure 4.

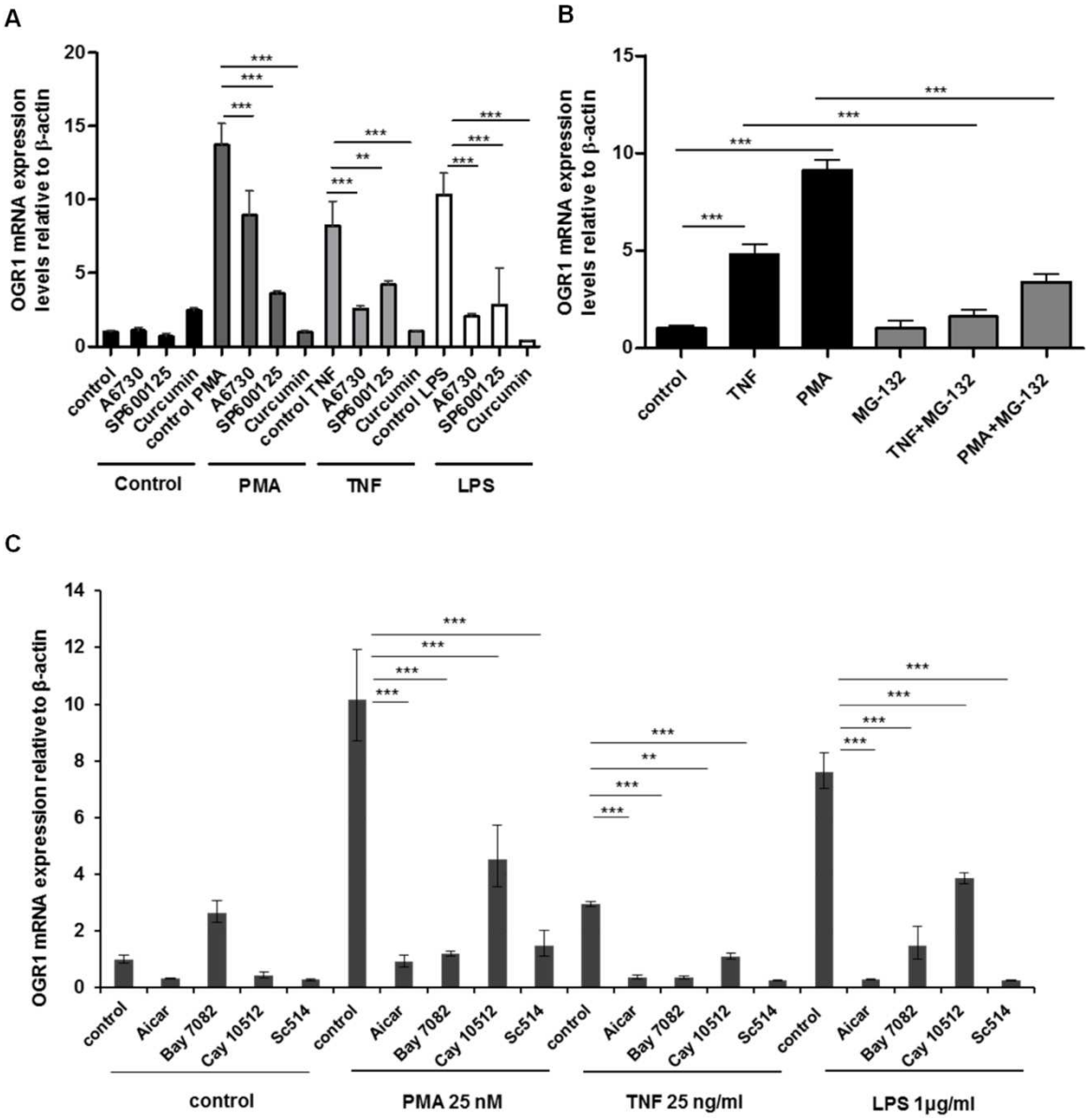
A
OGR1 mRNA expression levels relative to β-actin
control
A6730
SP600125
Curcumin
control PMA
control TNF
control LPS
Control
PMA
TNF
LPS
B
OGR1 mRNA expression levels relative to β-actin
control
TNF
PMA
MG-132
TNF+MG-132
PMA+MG-132
C
OGR1 mRNA expression relative to β-actin
control
Aicar
Bay 7082
Cay 10512
Sc514
control
PMA 25 nM
TNF 25 ng/ml
LPS 1µg/ml

Figure 5.

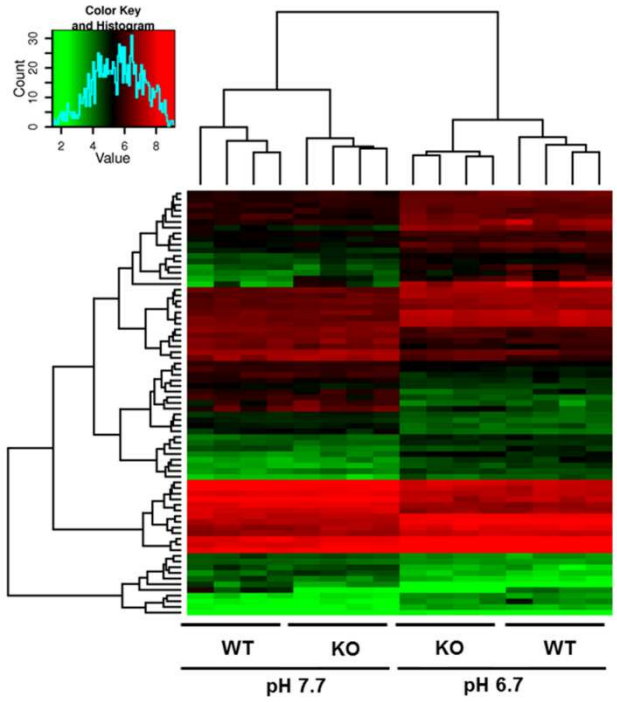
Color Key and Histogram
Count
Value
WT
KO
KO
WT
pH 7.7
pH 6.7

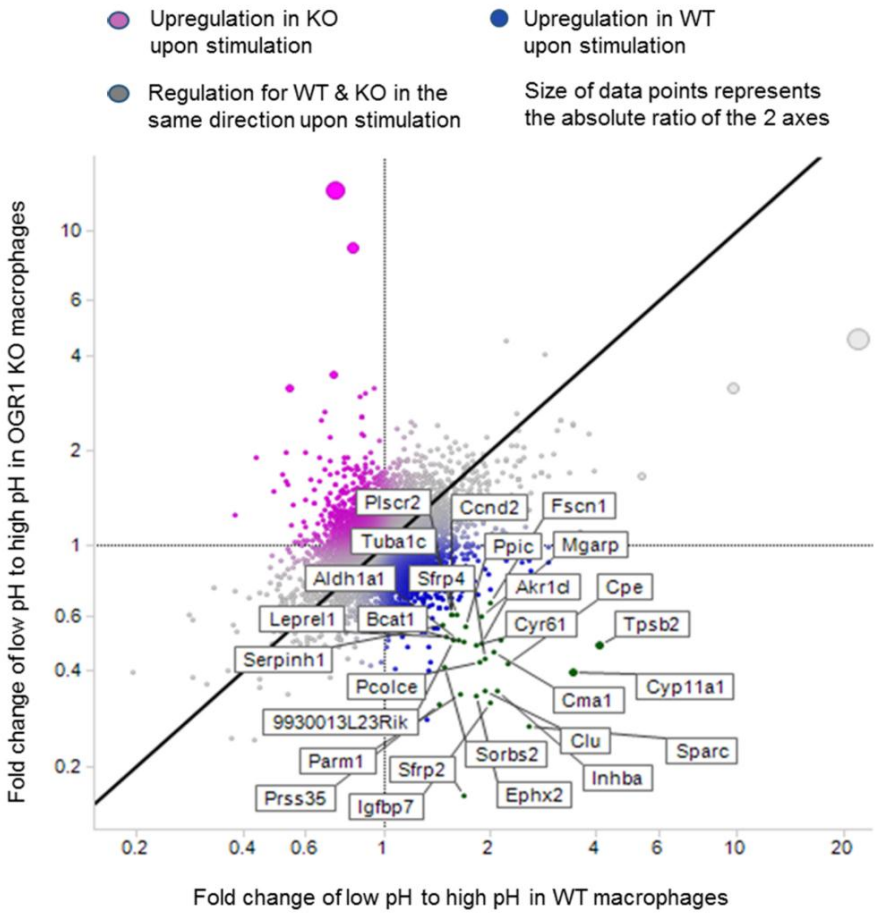
Upregulation in KO upon stimulation
Upregulation in WT upon stimulation
Regulation for WT & KO in the same direction upon stimulation
Size of data points represents the absolute ratio of the 2 axes
Fold change of low pH to high pH in OGR1 KO macrophages
Fold change of low pH to high pH in WT macrophages
Plscr2
Ccnd2
Fscn1
Tuba1c
Ppic
Mgarp
Aldh1a1
Sfrp4
Akr1d
Cpe
Leprel1
Bcat1
Cyr61
Tpsb2
Serpinh1
Pcolce
Cyp11a1
Cma1
9930013L23Rik
Clu
Parm1
Sorbs2
Sparc
Sfrp2
Inhba
Prss35
Igfbp7
Ephx2

Figure 6.

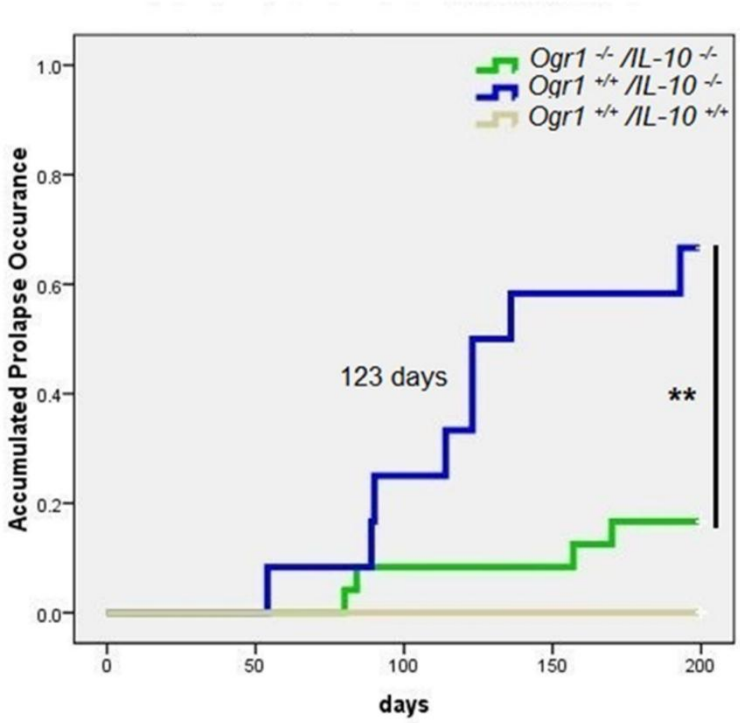

Figure 7.

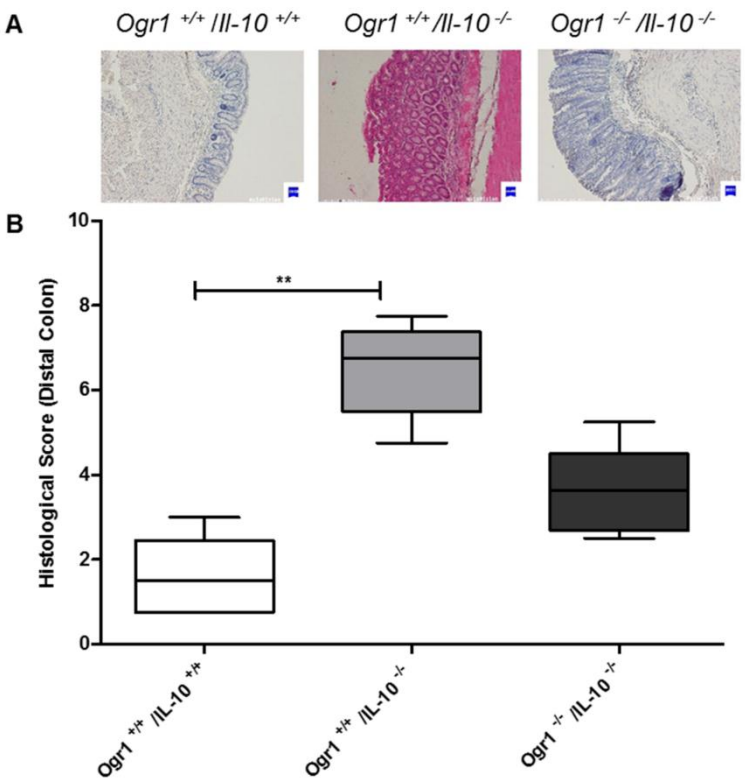

Figure 8.

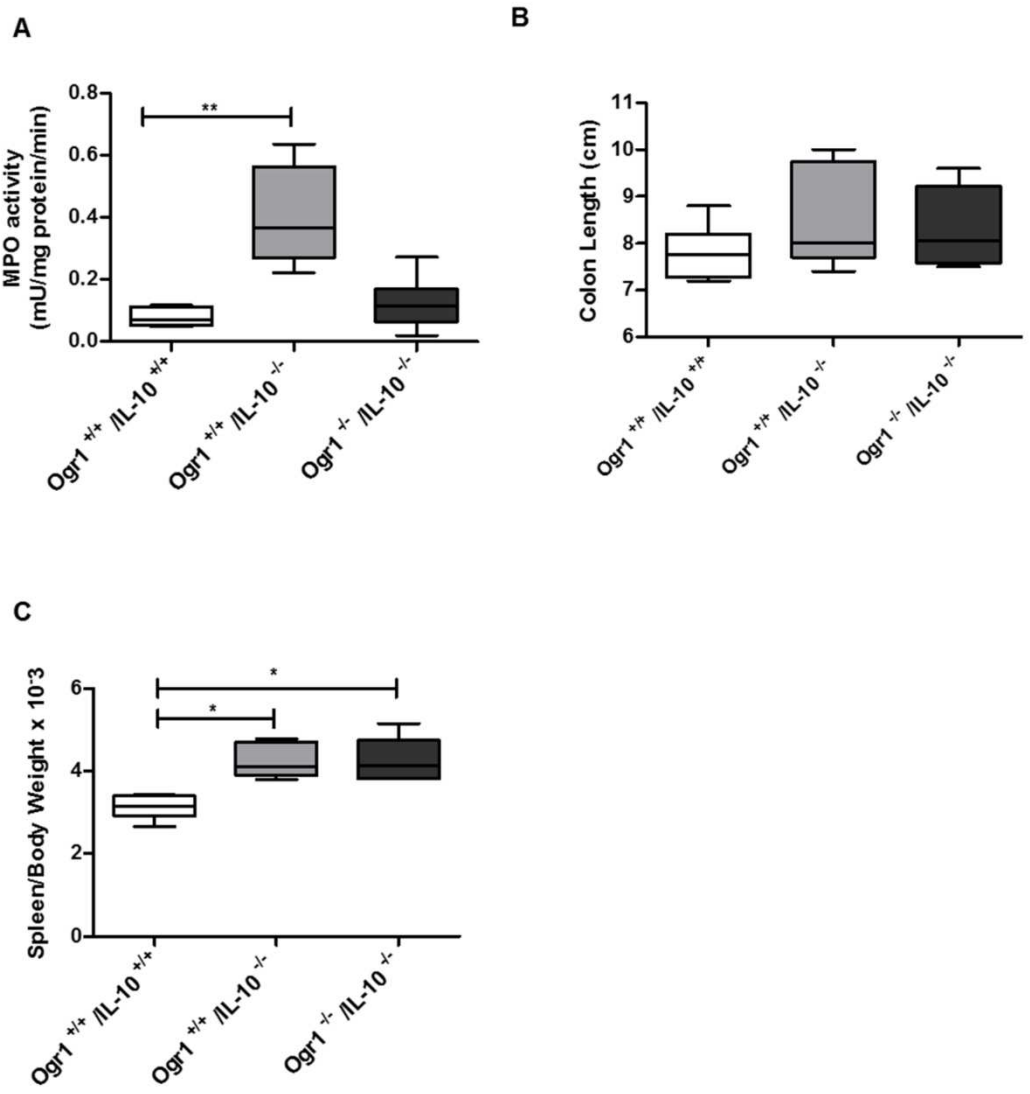
A
MPO activity (mU/mg protein/min)
0.8
0.6
0.4
0.2
0.0
**
Ogr1 +/+ /IL-10 +/+
Ogr1 +/+ /IL-10 -/-
Ogr1 -/- /IL-10 -/-
B
Colon Length (cm)
11
10
9
8
7
6
Ogr1 +/+ /IL-10 +/+
Ogr1 +/+ /IL-10 -/-
Ogr1 -/- /IL-10 -/-
C
Spleen/Body Weight x 10-3
6
4
2
0
*
*
Ogr1 +/+ /IL-10 +/+
Ogr1 +/+ /IL-10 -/-
Ogr1 -/- /IL-10 -/-

Figure 9.

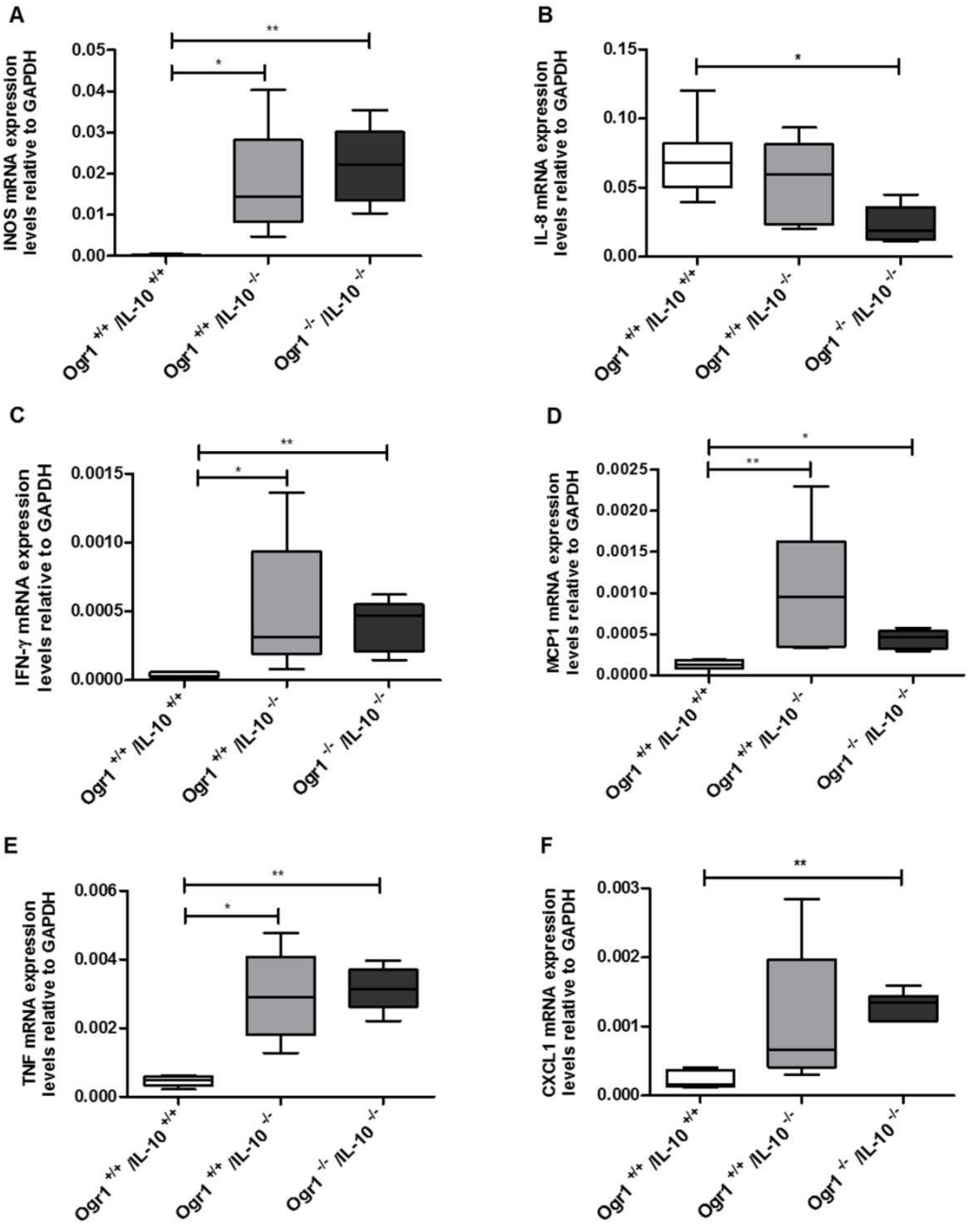
A
iNOS mRNA expression levels relative to GAPDH
0.05
0.04
0.03
0.02
0.01
0.00
**
*
Ogr1 +/+ /IL-10 +/+
Ogr1 +/+ /IL-10 -/-
Ogr1 -/- /IL-10 -/-
B
IL-8 mRNA expression levels relative to GAPDH
0.15
0.10
0.05
0.00
*
Ogr1 +/+ /IL-10 +/+
Ogr1 +/+ /IL-10 -/-
Ogr1 -/- /IL-10 -/-
C
IFN-γ mRNA expression levels relative to GAPDH
0.0015
0.0010
0.0005
0.0000
**
*
Ogr1 +/+ /IL-10 +/+
Ogr1 +/+ /IL-10 -/-
Ogr1 -/- /IL-10 -/-
D
MCP1 mRNA expression levels relative to GAPDH
0.0025
0.0020
0.0015
0.0010
0.0005
0.0000
*
**
Ogr1 +/+ /IL-10 +/+
Ogr1 +/+ /IL-10 -/-
Ogr1 -/- /IL-10 -/-
E
TNF mRNA expression levels relative to GAPDH
0.006
0.004
0.002
0.000
**
*
Ogr1 +/+ /IL-10 +/+
Ogr1 +/+ /IL-10 -/-
Ogr1 -/- /IL-10 -/-
F
CXCL1 mRNA expression levels relative to GAPDH
0.003
0.002
0.001
0.000
**
Ogr1 +/+ /IL-10 +/+
Ogr1 +/+ /IL-10 -/-
Ogr1 -/- /IL-10 -/-

Figure 10.

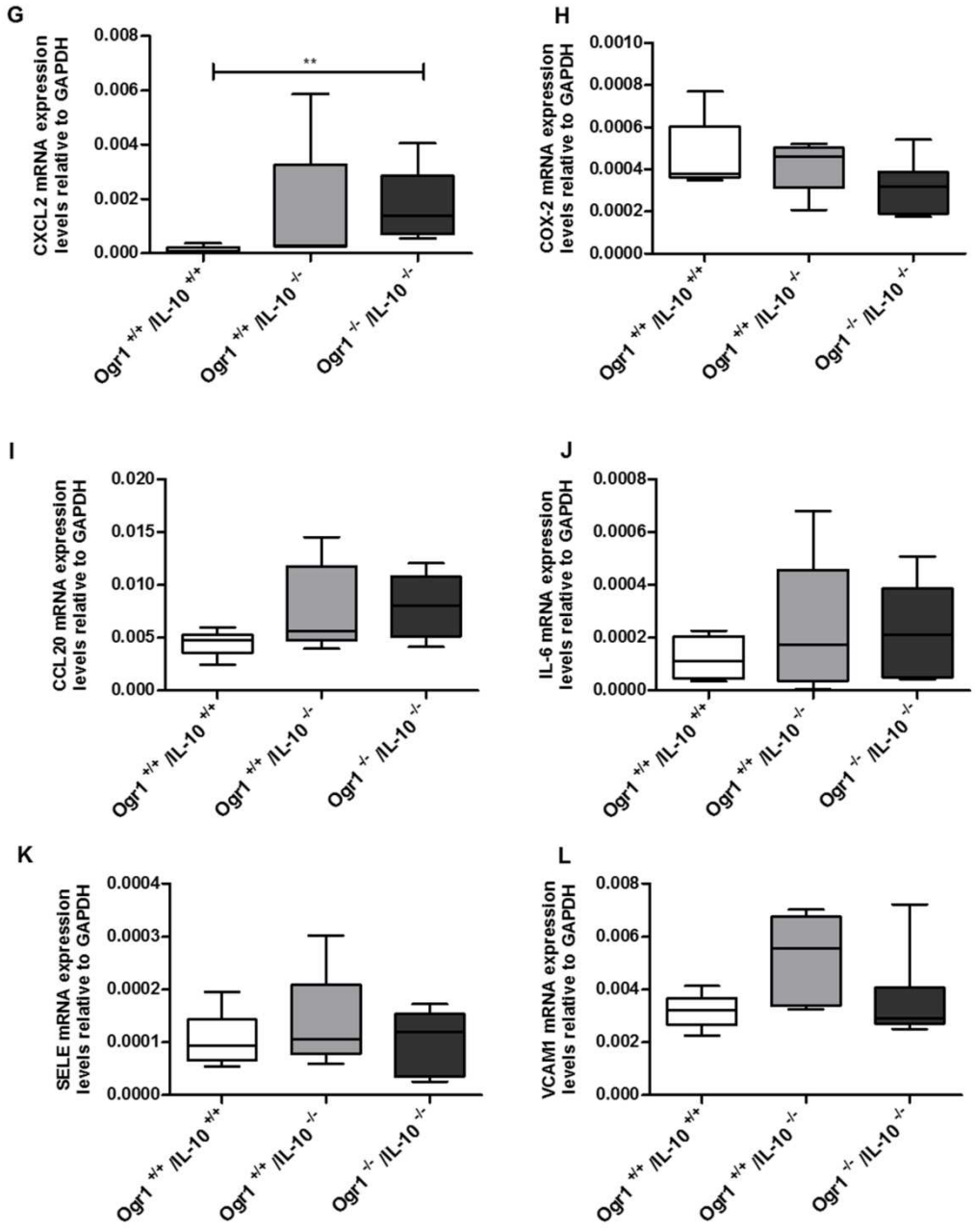
G
CXCL2 mRNA expression levels relative to GAPDH
0.008
0.006
0.004
0.002
0.000
**
Ogr1 +/+ /IL-10 +/+
Ogr1 +/+ /IL-10 -/-
Ogr1 -/- /IL-10 -/-
H
COX-2 mRNA expression levels relative to GAPDH
0.0010
0.0008
0.0006
0.0004
0.0002
0.0000
I
CCL20 mRNA expression levels relative to GAPDH
0.020
0.015
0.010
0.005
0.000
J
IL-6 mRNA expression levels relative to GAPDH
0.0008
0.0006
0.0004
0.0002
0.0000
K
SELE mRNA expression levels relative to GAPDH
0.0004
0.0003
0.0002
0.0001
0.0000
L
VCAM1 mRNA expression levels relative to GAPDH
0.008
0.006
0.004
0.002
0.000

Figure 10.

REFERENCES

1. Hanly EJ, Aurora AA, Shih SP, et al. Peritoneal acidosis mediates immunoprotection in laparoscopic surgery. Surgery 2007;142:357-64.
2. Mogi C, Tobo M, Tomura H, et al. Involvement of Proton-Sensing TDAG8 in Extracellular Acidification-Induced Inhibition of Proinflammatory Cytokine Production in Peritoneal Macrophages. Journal of Immunology 2009;182:3243-3251.
3. Brokelman WJ, Lensvelt M, Borel Rinkes IH, et al. Peritoneal changes due to laparoscopic surgery. Surg Endosc 2011;25:1-9.
4. Lardner A. The effects of extracellular pH on immune function. J Leukoc Biol 2001;69:522-30.
5. van Heel DA, Udalova IA, De Silva AP, et al. Inflammatory bowel disease is associated with functional TNF polymorphism affecting OCT1/NF-kappa B interaction. Gut 2002;50:A30-A30.
6. Sandborn WJ, Targan SR. Biologic therapy of inflammatory bowel disease. Gastroenterology 2002;122:1592-1608.
7. Blam ME, Stein RB, Lichtenstein GR. Integrating anti-tumor necrosis factor therapy in inflammatory bowel disease: current and future perspectives. Am J Gastroenterol 2001;96:1977-97.
8. Danese S, Colombel JF, Peyrin-Biroulet L, et al. Review article: the role of anti-TNF in the management of ulcerative colitis -- past, present and future. Aliment Pharmacol Ther 2013;37:855-66.
9. Rutgeerts PJ. Review article: efficacy of infliximab in Crohn's disease--induction and maintenance of remission. Aliment Pharmacol Ther 1999;13 Suppl 4:9-15; discussion 38.
10. van Dullemen HM, van Deventer SJ, Hommes DW, et al. Treatment of Crohn's disease with anti-tumor necrosis factor chimeric monoclonal antibody (cA2). Gastroenterology 1995;109:129-35.
11. Grivennikov SI, Tumanov AV, Liepinsh DJ, et al. Distinct and nonredundant in vivo functions of TNF produced by t cells and macrophages/neutrophils: protective and deleterious effects. Immunity 2005;22:93-104.
12. Neurath MF, Pettersson S, Meyer zum Buschenfelde KH, et al. Local administration of antisense phosphorothioate oligonucleotides to the p65 subunit of NF-kappa B abrogates established experimental colitis in mice. Nat Med 1996;2:998-1004.
13. Rogler G, Brand K, Vogl D, et al. Nuclear factor kappaB is activated in macrophages and epithelial cells of inflamed intestinal mucosa. Gastroenterology 1998;115:357-69.
14. Hatoum OA, Binion DG, Gutterman DD. Paradox of simultaneous intestinal ischaemia and hyperaemia in inflammatory bowel disease. Eur J Clin Invest 2005;35:599-609.
15. Ludwig MG, Vanek M, Guerini D, et al. Proton-sensing G-protein-coupled receptors. Nature 2003;425:93-8.
16. Seuwen K, Ludwig MG, Wolf RM. Receptors for protons or lipid messengers or both? J Recept Signal Transduct Res 2006;26:599-610.
17. Mogi C, Tomura H, Tobo M, et al. Sphingosylphosphorylcholine antagonizes proton-sensing ovarian cancer G-protein-coupled receptor 1 (OGR1)-mediated inositol phosphate production and cAMP accumulation. J Pharmacol Sci 2005;99:160-7.
18. Tomura H, Wang JQ, Komachi M, et al. Prostaglandin I(2) production and cAMP accumulation in response to acidic extracellular pH through OGR1 in human aortic smooth muscle cells. J Biol Chem 2005;280:34458-64.

19. Ichimonji I, Tomura H, Mogi C, et al. Extracellular acidification stimulates IL-6 production and Ca2+ mobilization through proton-sensing OGR1 receptors in human airway smooth muscle cells. American Journal of Physiology-Lung Cellular and Molecular Physiology 2010;299:L567-L577.
20. Palmer CD, Rahman FZ, Sewell GW, et al. Diminished macrophage apoptosis and reactive oxygen species generation after phorbol ester stimulation in Crohn's disease. PLoS One 2009;4:e7787.
21. Campos N, Magro F, Castro AR, et al. Macrophages from IBD patients exhibit defective tumour necrosis factor-alpha secretion but otherwise normal or augmented pro-inflammatory responses to infection. Immunobiology 2011;216:961-70.
22. Franke A, McGovern DP, Barrett JC, et al. Genome-wide meta-analysis increases to 71 the number of confirmed Crohn's disease susceptibility loci. Nat Genet 2010;42:1118-25.
23. Onozawa Y, Komai T, Oda T. Activation of T cell death-associated gene 8 attenuates inflammation by negatively regulating the function of inflammatory cells. Eur J Pharmacol 2011;654:315-9.
24. Wirtz S, Neurath MF. Mouse models of inflammatory bowel disease. Adv Drug Deliv Rev 2007;59:1073-83.
25. Solomon L, Mansor S, Mallon P, et al. The dextran sulphate sodium (DSS) model of colitis: an overview. Comparative Clinical Pathology 2010;19:235-239.
26. Hibi T, Ogata H, Sakuraba A. Animal models of inflammatory bowel disease. J Gastroenterol 2002;37:409-17.
27. Rogler G, Daig R, Aschenbrenner E, et al. Establishment of long-term primary cultures of human small and large intestinal epithelial cells. Lab Invest 1998;78:889-90.
28. Mohebbi N, Benabbas C, Vidal S, et al. The Proton-activated G Protein Coupled Receptor OGR1 Acutely Regulates the Activity of Epithelial Proton Transport Proteins. Cellular Physiology and Biochemistry 2012;29:313-324.
29. Zhang X, Goncalves R, Mosser DM. The isolation and characterization of murine macrophages. Curr Protoc Immunol 2008;Chapter 14:Unit 14 1.
30. Bentz S, Pesch T, Wolfram L, et al. Lack of transketolase-like (TKTL) 1 aggravates murine experimental colitis. Am J Physiol Gastrointest Liver Physiol 2011;300:G598-607.
31. Fischbeck A, Leucht K, Frey-Wagner I, et al. Sphingomyelin induces cathepsin D-mediated apoptosis in intestinal epithelial cells and increases inflammation in DSS colitis. Gut 2011;60:55-65.
32. Kauffmann A, Gentleman R, Huber W. arrayQualityMetrics--a bioconductor package for quality assessment of microarray data. Bioinformatics 2009;25:415-6.
33. Auwerx J. The human leukemia cell line, THP-1: a multifacetted model for the study of monocyte-macrophage differentiation. Experientia 1991;47:22-31.
34. Widmann C, Gibson S, Jarpe MB, et al. Mitogen-activated protein kinase: conservation of a three-kinase module from yeast to human. Physiol Rev 1999;79:143-80.
35. Seger R, Krebs EG. The MAPK signaling cascade. FASEB J 1995;9:726-35.
36. Cargnello M, Roux PP. Activation and function of the MAPKs and their substrates, the MAPK-activated protein kinases. Microbiol Mol Biol Rev 2011;75:50-83.
37. Angel P, Karin M. The role of Jun, Fos and the AP-1 complex in cell-proliferation and transformation. Biochim Biophys Acta 1991;1072:129-57.
38. Karin M. The regulation of AP-1 activity by mitogen-activated protein kinases. J Biol Chem 1995;270:16483-6.
39. DeFranco AL, Crowley MT, Finn A, et al. The role of tyrosine kinases and map kinases in LPS-induced signaling. Prog Clin Biol Res 1998;397:119-36.

40. Englaro W, Bahadoran P, Bertolotto C, et al. Tumor necrosis factor alpha-mediated inhibition of melanogenesis is dependent on nuclear factor kappa B activation. Oncogene 1999;18:1553-9.
41. Kane LP, Shapiro VS, Stokoe D, et al. Induction of NF-kappaB by the Akt/PKB kinase. Curr Biol 1999;9:601-4.
42. Ozes ON, Mayo LD, Gustin JA, et al. NF-kappaB activation by tumour necrosis factor requires the Akt serine-threonine kinase. Nature 1999;401:82-5.
43. Aggarwal BB, Kumar A, Bharti AC. Anticancer potential of curcumin: Preclinical and clinical studies. Anticancer Research 2003;23:363-398.
44. Aggarwal S, Ichikawa H, Takada Y, et al. Curcumin (diferuloylmethane) down-regulates expression of cell proliferation and antiapoptotic and metastatic gene products through suppression of IkappaBalpha kinase and Akt activation. Mol Pharmacol 2006;69:195-206.
45. Katerelos M, Mudge SJ, Stapleton D, et al. 5-aminoimidazole-4-carboxamide ribonucleoside and AMP-activated protein kinase inhibit signalling through NF-kappaB. Immunol Cell Biol 2010;88:754-60.
46. Pierce JW, Schoenleber R, Jesmok G, et al. Novel inhibitors of cytokine-induced IkappaBalpha phosphorylation and endothelial cell adhesion molecule expression show anti-inflammatory effects in vivo. J Biol Chem 1997;272:21096-103.
47. Kishore N, Sommers C, Mathialagan S, et al. A selective IKK-2 inhibitor blocks NF-kappa B-dependent gene expression in interleukin-1 beta-stimulated synovial fibroblasts. J Biol Chem 2003;278:32861-71.
48. Fujioka S, Niu J, Schmidt C, et al. NF-kappaB and AP-1 connection: mechanism of NF-kappaB-dependent regulation of AP-1 activity. Mol Cell Biol 2004;24:7806-19.
49. Cartharius K, Frech K, Grote K, et al. MatInspector and beyond: promoter analysis based on transcription factor binding sites. Bioinformatics 2005;21:2933-42.
50. Lum H, Qiao J, Walter RJ, et al. Inflammatory stress increases receptor for lysophosphatidylcholine in human microvascular endothelial cells. Am J Physiol Heart Circ Physiol 2003;285:H1786-9.
51. Haas JG, Baeuerle PA, Riethmuller G, et al. Molecular mechanisms in down-regulation of tumor necrosis factor expression. Proc Natl Acad Sci U S A 1990;87:9563-7.
52. Ziegler-Heitbrock HW, Blumenstein M, Kafferlein E, et al. In vitro desensitization to lipopolysaccharide suppresses tumour necrosis factor, interleukin-1 and interleukin-6 gene expression in a similar fashion. Immunology 1992;75:264-8.
53. Pei L, Castrillo A, Tontonoz P. Regulation of macrophage inflammatory gene expression by the orphan nuclear receptor Nur77. Mol Endocrinol 2006;20:786-94.
54. Esnault C, Stewart A, Gualdrini F, et al. Rho-actin signaling to the MRTF coactivators dominates the immediate transcriptional response to serum in fibroblasts. Genes Dev 2014;28:943-58.
55. Zhang YQ, Resta S, Jung B, et al. Upregulation of activin signaling in experimental colitis. Am J Physiol Gastrointest Liver Physiol 2009;297:G768-80.
56. Sierra-Filardi E, Puig-Kroger A, Blanco FJ, et al. Activin A skews macrophage polarization by promoting a proinflammatory phenotype and inhibiting the acquisition of anti-inflammatory macrophage markers. Blood 2011;117:5092-101.
57. Lin Z, Hegarty JP, Cappel JA, et al. Identification of disease-associated DNA methylation in intestinal tissues from patients with inflammatory bowel disease. Clin Genet 2011;80:59-67.
58. Karatzas PS, Gazouli M, Safioleas M, et al. DNA methylation changes in inflammatory bowel disease. Ann Gastroenterol 2014;27:125-132.

59. Ng YL, Klopcic B, Lloyd F, et al. Secreted protein acidic and rich in cysteine (SPARC) exacerbates colonic inflammatory symptoms in dextran sodium sulphate-induced murine colitis. PLoS One 2013;8:e77575.
60. Aljarari NMH. The role of GPCR on various second messenger systems. Journal of Basic Medical and Allied Sciences 2012:1-7.
61. Anderson CA, Boucher G, Lees CW, et al. Meta-analysis identifies 29 additional ulcerative colitis risk loci, increasing the number of confirmed associations to 47. Nat Genet 2011;43:246-52.
62. Jostins L, Ripke S, Weersma RK, et al. Host-microbe interactions have shaped the genetic architecture of inflammatory bowel disease. Nature 2012;491:119-24.
63. Khor B, Gardet A, Xavier RJ. Genetics and pathogenesis of inflammatory bowel disease. Nature 2011;474:307-17.

De Vallière et al.

Supplementary Material
The G protein-coupled pH-sensing receptor *OGR1* is a regulator of intestinal inflammation

Materials and Methods

Chemicals

Cytokines were obtained from Sigma-Aldrich (St. Louis, MA, USA), unless otherwise stated. TNF (#654205) was purchased from Calbiochem (Merck Darmstadt, Germany). 5-aminoimidazole-4-carboxamide-1-beta-4-ribofuranoside (AICAR) (#100102-41), BAY-11-7082 (#100010266), CAY10512 (#10009536), Curcumin (#81025.1), SC-514 (Cayman#10010267), SP600125 (Cayman #100010466) were purchased from Cayman (Ann Arbor, Michigan, USA).

Genomic DNA extraction and genotyping

For PCR reactions, the oligonucleotides used were as follows:
Il-10 genotyping: 5'-GTGGGTGCAGTTATTGTCTTCCCG-3' (oIMR0086),
5'-GCCTTCAGTATAAAAGGGGGACC-3' (oIMR0087),
5'-CCTGCGTGCAATCCATCTTG-3' (oIMR0088),
Ogr-1 genotyping:
5'-ACCACC AGTGATGCCTAGATCCTG A-3' (P416),
5'-AAGATGACCACGGTGCTGAGC ACC A-3' (P417),
5'-CCATTCGACCACCAAGCG AAACAT C-3' (R3).

Murine macrophage isolation and culture

Peritoneal murine macrophages were centrifuged, washed in PBS and resuspended in RPMI 1640 medium containing 2 mM Glutamax (35050-038, Gibco), 10% fetal calf serum (2-01F120-I, Amimed, Bio Concept, Allschwil, Switzerland), 100 U/ml penicillin, 100

µg/ml streptomycin (all obtained from Sigma–Aldrich, Buchs, Switzerland). Cells from each mouse were treated without pooling, after plating in 6 well plates (≈ 3 x 10^6 cells in 1 ml/well) at 37°C, 5% CO_2. After 2 h, non-adherent cells were removed. Macrophages were maintained in RPMI medium, 5% CO_2 for 24 h. Final number of cells per treatment (obtained from each mouse) was ≈ 1 x 10^6 cells. The resulting adherent population consisted of ≈ 88% peritoneal macrophages as determined by flow cytometry (data not shown).

RNA extraction and quantitative Real-Time RT-PCR.

Human and mouse tissue.

Tissue pieces used for RNA analysis were transferred immediately into RNAlater solution (Qiagen, Valencia, CA) and stored at −80°C. Tissue biopsies were disrupted in RLT buffer (Qiagen) using a 26G needle.

Cells and tissue samples. Total RNA was isolated using the RNeasy Mini Kit in the automated QIAcube following the manufacturer's recommendations (Qiagen, Hombrechtikon, Switzerland). For removal of residual DNA, DNase treatment, 15 min at room temperature, was integrated into the QIAcube program according to the manufacturer's instructions. For cDNA synthesis, the High-Capacity cDNA Reverse Transcription Kit (Applied Biosystems, Foster City, CA), was used, following the manufacturer's instructions. Determination of mRNA expression was performed by quantitative real-time PCR (qRT-PCR) on a 7900HT real-time PCR system (Applied Biosystems, Foster City, USA), under the following cycling conditions: 20 sec at 95 °C, then 45 cycles of 95 °C for 3 sec and 60 °C for 30 sec with the TaqMan Fast Universal Mastermix. Samples were analyzed as triplicates. Relative mRNA expression was determined the by the comparative ΔΔCt method[1], which calculates the quantity of the target sequences relative to the endogenous control and a reference sample. TAQMAN Gene Expression Assays, (all from Applied Biosystems, Foster City, USA), used in this study are listed in the online supplementary Table S1.

Table S1. TaqMan assays

Gene Symbol	Gene Name	Assay ID
GPR68	Human G protein-coupled receptor 68, *OGR1*	Hs 00268858- s1
GPR4	Human G protein-coupled receptor 4	Hs 00270999 - s1
GPR65	Human G protein-coupled receptor 65, *TDAG8*	Hs 00269247 - s1
GAPDH	Human glyceraldehyde-3-phosphate dehydrogenase (GAPDH) Endogenous Control	4326317E
ACTB	Human ACTB (beta actin) Endogenous Control	4310881E
HuPo	Human acidic ribosomal protein (RPLPO) Endogenous Control	4310879E
HPRT1	Human Hypoxanthine guanine phosphoribosyl transferase 1	Hs01003268_g1
GPR68	Mouse G protein-coupled receptor 68, *OGR1*	Mm00558545_s1
GPR4	Mouse G protein-coupled receptor 4	Mm00558777_s1
GPR65	Mouse G protein-coupled receptor 65, *TDAG8*	Mm00433695_m1
CCL20	Mouse chemokine (C-C motif) ligand 20	Mm01268754_m1
COX-2	Mouse prostaglandin-endoperoxide synthase 2	Mm00478374_m1
CXCL1	Mouse chemokine (C-X-C motif) ligand 1	Mm04207460_m1
CXCL2	Mouse chemokine (C-X-C motif) ligand 2	Mm00436450_m1
IFN-γ	Mouse interferon gamma	Mm00801778_m1
IL-18	Mouse Interleukin 18	Mm00434225_m1
IL-6	Mouse Interleukin 6	Mm00446190_m1
iNOS	Mouse nitric oxide synthase 2	Mm01309893_m1
MCP-1	Mouse chemokine (C-C motif) ligand 2	Mm00441242_m1
SELE	Mouse selectin, endothelial cell	Mm00441278_m1
TNF-α	Mouse tumour necrosis factor alpha	Mm99999068_m1
VCAM1	Mouse vascular cell adhesion molecule 1	Mm01320970_m1
GAPDH	Mouse glyceraldehyde-3-phosphate dehydrogenase (GAPDH) Endogenous Control	Mm03302249_g1

Human β-actin 4310881E, Human hupo, 4310879E, Human GAPDH 4326317E, Human HPRT1 (hypoxanthine phosphoribosyltransferase 1) Hs01003268_g1 Cat. # 4331182
Human HuPo/ RPLP0 (large ribosomal protein) Endogenous Control (VIC / TAMRA Probe, Primer Limited), 4310879E, Human acidic ribosomal protein (HuPO), Hypoxanthine guanine phosphoribosyl transferase

Predictive location of OGR1 Promoter Variants 1 and 2 on Chromosome 14

Human G protein-coupled receptor 68 (GPR68), transcript variant 1, mRNA 2,880 bp linear mRNA
Human G protein-coupled receptor 68 (GPR68), transcript variant 2, mRNA 2,834 bp linear mRNA

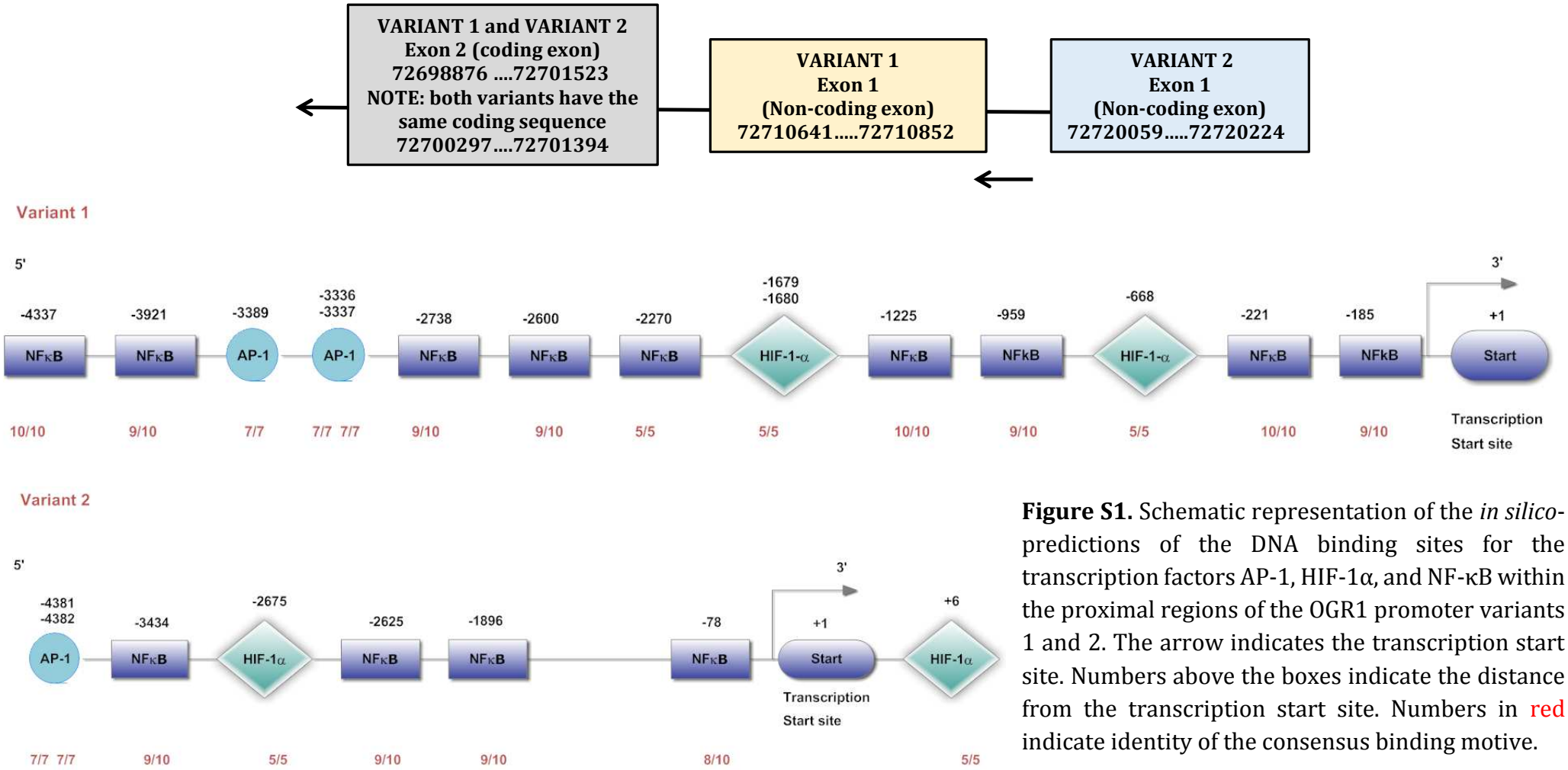

Figure S1. Schematic representation of the *in silico*-predictions of the DNA binding sites for the transcription factors AP-1, HIF-1α, and NF-κB within the proximal regions of the OGR1 promoter variants 1 and 2. The arrow indicates the transcription start site. Numbers above the boxes indicate the distance from the transcription start site. Numbers in red indicate identity of the consensus binding motive.

NFκB: 5' GGGRNYYYCC 3'

R = purine (A or G), Y = pyrimidine (T or C), N = any

- 396 (+) caGCGActtcccgca 9/10 -185
- 432 (-) ctggggatTTTCtag 10/10 -221
- 1170 (-) ctgggcctTTCCatc 9/10 -959
- 1436 (-) aaggggatTTCCtta 10/10 -1225
- 2481 (+) caGGGAttatcctgt 9/10 -2270
- 2811 (+) gagatgGGATttctc 9/10 -2600
- 2949 (+) atggggttTTGCcat 9/10 -2738
- 4132 (+) gatgggatTTCAccg 9/10 - 3921
- 4548 (-) aaGGGAtcctccctt 10/10 – 4337

(subtract 211 to obtain the location from the transcription start site)

HRE: 5' (A/G)CGTG 3'

- 879 (+) ggaagtgaCGTGccagc 5/5 -668
- 1890 (+) tagacacaCGTGctact 5/5 -1679
- 1891 (+) aagtagcaCGTGtgtct 5/5 -1680
- 3417 (-) ttaccttaCGTGgcaaa 5/5 -3206

(subtract 211 to obtain the location from the transcription start site)

AP-1: 5' TGACTCA 3'

- 85 (-) cattcaTGGGtcagtaaatca
- 98 (+) catgaaTGGGtcacaacccgc
- 1598 (-) ccGGCCtggtc
- 1972 (-) cactGCTAagtcagttctgtg
- 1974 (+) cagaacTGACttagcagtgac
- 2263 (-) atttGAGTaaaac
- 2300 (-) tcttacTGAGctagcatttca
- 2330 (-) agcacaTGAGagagcatgggc
- 2769 (+) caggcaTGTGtcactatgcct
- 3346 (+) caatGCTGgatcactccttac
- 3366 (-) cctaatcagCTGAccttaaag
- 3546 (-) taggcaTGAGtcacctcaccc
- 3547 (-) gcatgAGTCacct 7/7 3336
- 3547 (+) aggTGACtcatgc
- 3548 (+) gtgagGTGActcatgcctata 7/7 3337
- 3599 (-) aaacccTGAGtcaagcaatcc
- 3600 (+) gctTGACtcaggg 7/7 3389
- 3600 (-) cccTGAGtcaagc
- 3797 (+) aaaccaTGTGtcaagcaaaac
- 4901 (+) tgatgcCTCAcag
- 5162 (-) ggaGGCTgaggcggcaggatt

(subtract 211 to obtain position from transcription start site)

Figure S2. List of possible binding sites to the consensus elements AP-1, HIF1-α and NFκB in the *in silico* promoter analysis of OGR1.

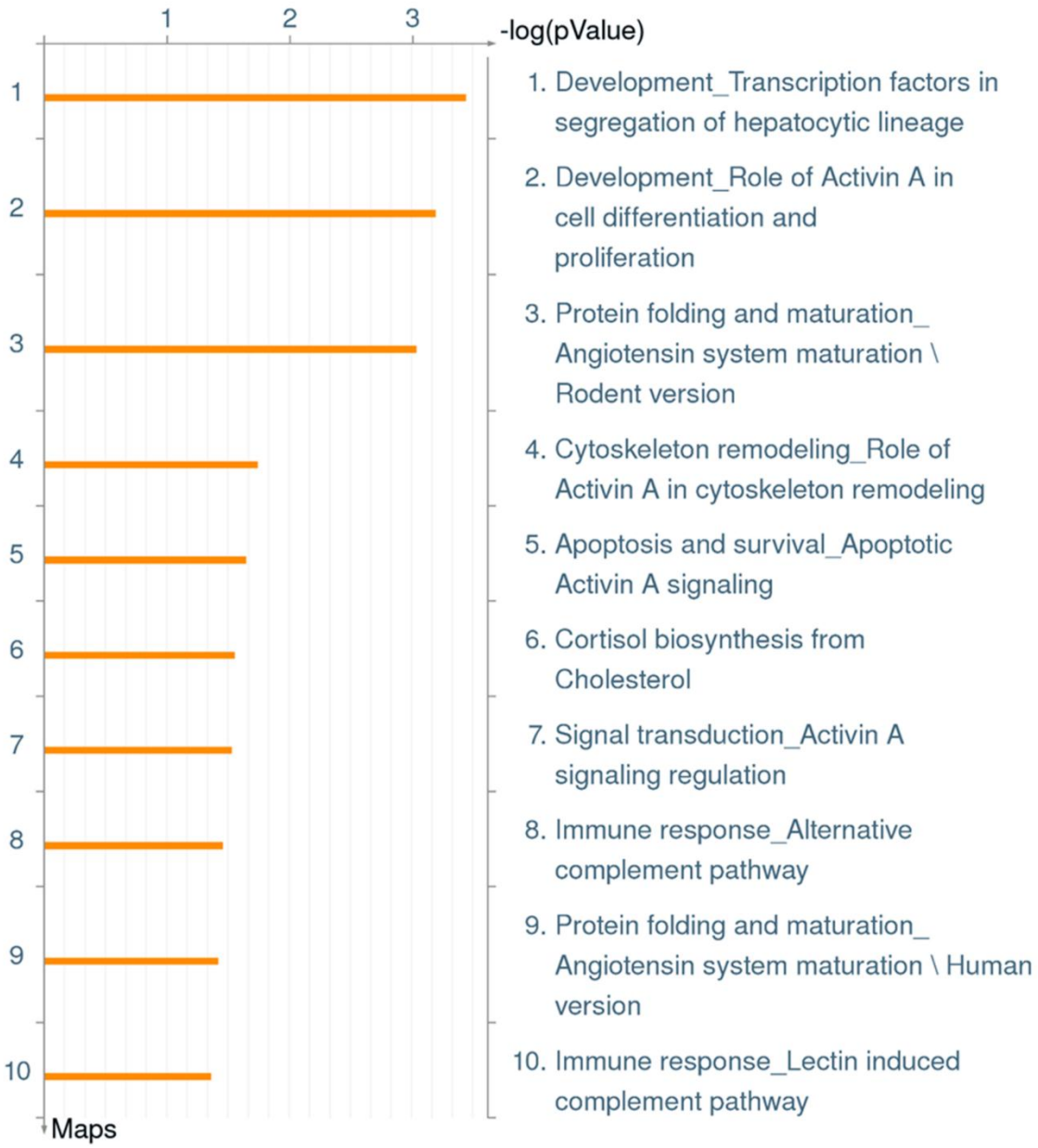

Figure S3. Enrichment analysis: Meta Core (Gene Go) Pathway Maps Ontology. Pairwise comparison of acidified WT vs. Ogr1 KO murine macrophages. pH 6.7 24 h. Extracellular acidosis activation of *Ogr1* in murine macrophages show that the most significantly enriched canonical pathways include Activin A associated pathways, immune response and actin cytoskeleton remodeling pathways.

Table S2.A-B. Differentially expressed genes following activation of OGR1 by acidic pH in mouse peritoneal macrophages pH 6.7 24 h. **A.** Gene List, including gene process **B.** Complete Table (Excel).

Rank WT/KO Ratio	Symbol	Full name	Involved in: (Reference: Gene Card, NCBI, JAX, Uniprot, unless otherwise indicated)
1.	*Cyp11a1*	Cholesterol side chain cleavage enzyme, mitochondrial (Cytochrome P450 11A1)	Cholesterol, lipid or steroid metabolism. Catalyses the side-chain cleavage reaction of cholesterol to pregnenolone.
2.	*Sparc*	Secreted acidic cysteine rich glycoprotein (Osteonectin, Basement membrane protein 40 (BM-40))	Cell adhesion, wound healing, ECM interactions, bone mineralization. Activates production and activity of matrix metalloproteinases.
3.	*Tpsb2*	Tryptase beta-2 or tryptase II (trypsin-like serine protease)	Inflammatory response, proteolysis.
4.	*Inhba*	Inhibin Beta A or Activin beta-A chain	Immune response and mediators of inflammation and tissue repair.[2-5]
5.	*Cpe*	Carboxypeptidase E	Insulin processing, proteolysis.
6.	*Igfbp7*	Insulin-like growth factor-binding protein 7	Stimulates prostacyclin (PGI2) production and cell adhesion. Induced by retinoic acid.
7.	*Clu*	Clusterin	Chaperone-mediated protein folding, positive regulation of NF-κB transcription factor activity. Protects cells against apoptosis and cytolysis by complement. Promotes proteasomal degradation of COMMD1 and IKBKB.
8.	*Cma1*	Chymase 1	Cellular response to glucose stimulus, interleukin-1 beta biosynthetic process. Possible roles: vasoactive peptide generation, extracellular matrix degradation.
9.	*Sfrp4*	Secreted frizzled-related protein 4	Negative regulation of Wnt signalling. Increases apoptosis during ovulation. Phosphaturic effects by specifically inhibiting sodium-dependent phosphate uptake.
10.	*Ephx2*	Bifunctional epoxide hydrolase	Cholesterol homeostasis, xenobiotic metabolism by degrading potentially toxic epoxides.
11.	*Pcolce*	Procollagen C-endopeptidase enhancer	Proteolysis. Collagen binding. Component in collagen and extracellular matrix.
12.	*Akr1cl*	Aldo-keto reductase family 1, member C-like	Oxidoreductase activity
13.	*Cyr61*	Cysteine rich protein 61	Cell adhesion, chemotaxis, cell proliferation, wound healing and angiogenesis.
14.	*Sfrp2*	Secreted frizzled-related protein 2	Differentiation, modulator of Wnt signalling pathway.
15.	*Parm1*	Prostate androgen-regulated mucin-like protein 1	Regulation of TLP1 expression and telomerase activity, enabling certain prostatic cells to resist apoptosis.
16.	*Bcat1*	Branched chain aminotransferase 1	Branched-chain amino acid biosynthetic process.
17.	*Mgarp*	Mitochondria localized glutamic acid rich protein, Hypoxia up-regulated mitochondrial movement regulator protein	Response to steroid hormone stimulus & hypoxia. Trafficking of mitochondria along microtubules. Aids steroidogenesis through maintenance of mitochondrial abundance & morphology.

18.	*Ppic*	Peptidyl-prolyl cis-trans isomerase C, cyclophilin C, cyp-20c	Accelerates protein folding.
19.	*Aldh1a1*	Retinal dehydrogenase 1, aldehyde dehydrogenase family 1, A1	9-cis-retinoic acid biosynthetic process. Converts/oxidizes retinaldehyde to retinoic acid.
20.	*9930013L 23RikCemi p*	Cell migration inducing protein	ER retention sequence binding, hyaluronic acid binding,
21.	*Fscn1*	Fascin homolog 1, actin bundling protein	Actin filament bundle assembly, cell migration. Organization of actin filament bundles, formation of microspikes, membrane ruffles, and stress fibres. Associates with beta-catenin.
22.	*Sorbs2*	Sorbin and SH3 domain containing 2	Actin filament organization, cell adhesion, cell migration.
23.	*Tuba1c*	Tubulin, alpha 1C	Microtubule-based process.
24.	*Leprel1*	Prolyl 3-hydroxylase 2 leprecan-like protein 1	Collagen metabolic process, negative regulation of cell proliferation.
25.	*Prss35*	Inactive serine protease 35	Serine protease homolog.
26.	*Plscr2*	Phospholipid scramblase 2	Cellular response to lipopolysaccharide.
27.	*Ccnd2*	Cyclin D2	Cell cycle, cell division, protein kinase binding.
28.	*Serpinh1*	Serpin H1	Stress response. Binds specifically to collagen. May be involved as a chaperone in the biosynthetic pathway of collagen.
29.	*Iglv1*	Immunoglobulin lambda variable 1	Immune Response
30.	*Tnfrsf13c*	Tumour necrosis factor receptor superfamily, member 13c	B, T cell costimulation, positive regulation of B and T cell proliferation, positive regulation of interferon-gamma biosynthetic process.
31.	*Timp1*	Metalloproteinase inhibitor 1, tissue inhibitor of metallo-proteinase 1	Response to cytokine, negative regulation of apoptotic process, wound healing. Complexes with metalloproteinases (such as collagenases) and irreversibly inactivates them by binding to their catalytic zinc cofactor.
32.	*Rpl18a*	Ribosomal protein L18A	Translation
33.	*Cd79a*	CD79A antigen (immunoglobulin-associated alpha)	Immune response
34.	*Ccl24*	Chemokine (C-C motif) ligand 24	Chemotaxis, Inflammatory response, cytoskeleton organization
35.	*Nrbf2*	Nuclear receptor (NR) binding factor 2	Transcription, transcription regulation. May modulate transcriptional activation by target NRs.
36.	*Gm9513*	Predicted gene 9513, Secreted tfp/ly-6/upar protein pate-p	N/A
37.	*Rpl35a*	Ribosomal protein L35A	rRNA processing
38.	*1700022K RikN4bp2 os*	NEDD4 binding protein 2, opposite strand	N/A
39.	*H2-Eb1*	Histocompatibility 2, class II antigen E beta	Antigen processing and presentation of exogenous peptide antigen via MHC class II.
40.	*Map1b*	Microtubule-associated protein 1B	Microtubule bundle formation, actin binding, cytoskeletal regulatory protein binding.
41.	*Nrn1*	Neuritin 1	Axonogenesis
42.	*Tinagl1*	Tubulointerstitial nephritis antigen-like 1	Immune response, proteolysis, cysteine-type peptidase activity, laminin binding.
43.	*Gm11937*	Predicted gene 11937	Fibrous proteins rich in cysteine, keratin.
44.	*Olfr1004p s1*	Olfactory receptor 1004, pseudogene 1	Olfactory receptor

45.	*Cxcl13*	Chemokine (C-X-C motif) ligand 13	Chemotaxis, Inflammatory response.
46.	*Htra1*	Htra serine peptidase 1 or insulin-like growth factor binding protein 5 protease	Negative regulation of defense response to virus, TGFβ receptor and BMP signalling pathway
47.	*Parva*	Parvin, alpha	Actin cytoskeleton reorganization, actin-mediated cell contraction, cell polarity, substrate adhesion-dependent cell spreading, directed cell migration.
48.	*Aebp1*	AE binding protein 1, Adipocyte enhancer-binding protein 1	Cell adhesion, proteolysis. Isoform 2 may positively regulate NF-κB activity in macrophages by promoting phosphorylation and degradation of Iκ-B-α (NFKBIA), leading to enhanced macrophage inflammatory responsiveness.
49.	*Lst1*	Leukocyte specific transcript 1	Cell shape, immune response. Induces filopodia and microspikes, may be involved in dendritic cell maturation
50.	*Psmb5-ps*	Proteasome (prosome, macropain) subunit, beta type 5, pseudogene	Proteasome-mediated ubiquitin-dependent protein catabolic process, response to oxidative stress.
51.	*Trav13-2*	T cell receptor alpha variable 13-2	
52.	*Krtap6-2*	Keratin associated protein 6-2	Hair keratin-associated protein gene
53.	*Kcng2*	Potassium voltage-gated channel, subfamily G, member 2	Potassium ion transmembrane transport
54.	*Dab2*	Disabled 2, mitogen-responsive phosphoprotein	Apoptosis, Differentiation, Endocytosis, Protein transport, Transport, Wnt signalling.
55.	*Atp2a3*	Endoplasmic reticulum (ER) Ca^{2+} ATPase 3	Ca^{2+} transport, ion transport. Mg^{2+}-dependent enzyme, catalyses hydrolysis of ATP coupled with transport of Ca^{2+}. Transports Ca^{2+} from cytosol into sarcoplasmic/ER lumen
56.	*Siglec1*	Sialic acid binding Ig-like lectin 1, sialoadhesin	Cell adhesion, endocytosis
57.	*Gm6816 (Rps4lps)*	Ribosomal protein S4-like, pseudogene	Translation
58.	*Mmp11*	Matrix metallopeptidase 11	Basement membrane organization, Ca^{2} binding, metalloendopeptidase activity, Zn^{2+}-binding
59.	*Fdx1*	Ferredoxin 1	Cholesterol metabolic process, hormone biosynthetic process
60.	*Adamts1*	ADAM metallopeptidase with thrombospondin type 1 motif, 1	Inflammatory response
61.	*Fbxo32*	F-box protein 32	Protein ubiquitination
62.	*Uck2*	Uridine-cytidine kinase 2	UMP, CTP salvage, cellular response to oxygen levels.
63.	*Tm4sf19*	Transmembrane 4 L six family member 19	N/A
64.	*Gm10334*	Predicted gene 10334	Proteolysis
65.	*Rps2-ps13*	Ribosomal protein S2, pseudogene 13	N/A
66.	*Slc16a2*	Solute carrier family 16 (monocarboxylic acid transporters), member 2	Symporter activity
67.	*Cdh2*	Cadherin-2	Cell adhesion, calcium-dependent.
68.	*Gm13375*	Predicted gene 13375	N/A

69.	*Kifc5b*	Kinesin family member C5B	Microtubule binding and microtubule motor activity.
70.	*Slc7a8*	Solute carrier family 7 (cationic amino acid transporter, y+ system) member 8	Large and neutral amino acid transmembrane transport.
71.	*C1qa*	Complement component 1, q subcomponent, alpha polypeptide	Complement activation, classical pathway, immune system process,
72.	*Gm10540*	Predicted gene 10540	N/A
73.	*Gm10153*	Predicted gene 10153	N/A
74.	*Tsga10ip*	Testis specific 10 interacting protein	N/A
75.	*Cir1*	Corepressor interacting with RBPJ, 1 Recombining binding proteinsuppressor of hairless	Required for RBPJ-mediated repression of transcription
76.	*Hmgb3*	High mobility group box 3	Negative regulation of myeloid cell differentiation
77.	*Ormdl3*	ORM1-like 3	Ceramide metabolic process. Negative regulator of sphingolipid synthesis. May indirectly regulate endoplasmic reticulum-mediated calcium signalling
78.	*5430421N 21Rik*	RIKEN cdna 5430421N21 gene	Human homolog KRT83, keratin 83, intermediate filament (cytoskeleton)
79.	*Krt8*	Keratin, type II cytoskeletal 8, cytokeratin8	Maintains cellular structural integrity and cellular differentiation. TNF-mediated signalling pathway.
80.	*Cnn3*	Calponin 3, acidic	Thin filament-associated protein. Binds to actin, calmodulin, troponin C and tropomyosin. Interaction of calponin with actin inhibits actomyosin Mg-ATPase activity.
81.	*Acsf2*	Acyl-CoA synthetase family member 2	Acyl-CoA synthases catalyze the initial reaction in fatty acid metabolism.
82.	*F2r*	F2r coagulation factor II (thrombin) receptor, (Proteinase-activated receptor 1 (PAR1))	Regulation of thrombotic response.
83.	*C1qb*	C1qb complement component 1, q subcomponent, beta polypeptide	Immune and stress response.
84.	*Cd83*	CD83 antigen	Immune response, antigen presentation and cellular interactions that follow lymphocyte activation
85.	*Vmn2r4*	Vomeronasal 2, receptor 4	GPCR, putative pheromone receptor.
86.	*Hs6st2*	Heparan sulfate 6-O-sulfotransferase 2	Heparan sulfate proteoglycans are molecules in cell surface, ECM & basement membranes. Involved in cell growth, differentiation, adhesion, and migration. *Hs6st2* catalyzes the transfer of sulfate to HS.
87.	*Gm9025*	Predicted gene 9025	
88.	*H2-Aa*	H2-Aa histocompatibility 2, class II antigen A, alpha	Immune response
89.	*Vmn1r59*	Vomeronasal 1 receptor 59	GPCR, pheromone receptor.
90.	*Serpine2*	Serpine2 serine (or cysteine) peptidase inhibitor, clade E, member 2	Serine protease inhibitor with activity toward thrombin, trypsin, and urokinase. Promotes neurite extension by inhibiting thrombin. Binds heparin.
91.	*Hsd3b1*	Hydroxy-delta-5-steroid dehydrogenase, 3 beta- and steroid delta-isomerase 1	Possible steroid biosynthetic process

92.	*Ube2c*	Ubiquitin-conjugating enzyme E2C	Ubiquitin-protein ligase activity
93.	*Mcpt4*	Mast cell protease 4	Proteolysis
94.	*Tgm2*	Transglutaminase 2, C polypeptide	Protein crosslinking
95.	*Ptgs1*	Prostaglandin-endoperoxide synthase 1 (COX-1)	
96.	*Txlng*	Taxilin gamma	Intracellular vesicle trafficking
97.	*Igkv8-30*	Immunoglobulin kappa chain variable 8-30	Immune response
98.	*Lsm6*	Lsm6 homolog, U6 small nuclear RNA associated (S. cerevisiae)	Involved in RNA processing
99.	*Gm4968*	Predicted gene 4968	
100.	*Ccl17*	Chemokine (C-C motif) ligand 17	Induces chemotaxis in T cells

Table S2.B. Differentially expressed genes following activation of OGR1 by acidic pH in mouse peritoneal macrophages (pH 6.7 24 h). Fold change WT pH 6.7 compared to control pH 7.7. KO fold change WT pH 6.7 compared to control pH 7.7

ID	Associated Gene Name	MGI symbol	Entrez Gene ID	WT vs KO rank	KO_ratio	WT_ratio	KO rank	WT rank	rank dif
ENSMUSG00000032323	Cyp11a1	Cyp11a1	13070	1	0.3965	3.443	23062	8	-23054
ENSMUSG00000018593	Sparc	Sparc	20692	2	0.2669	2.584	23077	29	-23048
ENSMUSG00000033825	Tpsb2	Tpsb2	17229	3	0.4862	4.052	23034	4	-23030
ENSMUSG00000041324	Inhba	Inhba	16323	4	0.3477	2.096	23069	74	-22995
ENSMUSG00000037852	Cpe	Cpe	12876	5	0.4238	2.239	23052	61	-22991
ENSMUSG00000036256	Igfbp7	Igfbp7	29817	5	0.3177	1.994	23074	83	-22991
ENSMUSG00000022037	Clu	Clu	12759	7	0.3458	1.937	23070	98	-22972
ENSMUSG00000022225	Cma1	Cma1	17228	8	0.4597	2.036	23044	79	-22965
ENSMUSG00000021319	Sfrp4	Sfrp4	20379	9	0.4407	1.941	23046	96	-22950
ENSMUSG00000022040	Ephx2	Ephx2	13850	10	0.333	1.827	23073	126	-22947
ENSMUSG00000048648	Gm9830	predicted gene 9830		11	0.5033	2.134	23011	70	-22941
ENSMUSG00000029718	Pcolce	Pcolce	18542	12	0.4269	1.864	23051	116	-22935
ENSMUSG00000025955	Akr1cl	Akr1cl	70861	13	0.4894	1.887	23031	110	-22921
ENSMUSG00000028195	Cyr61	Cyr61	16007	14	0.4826	1.824	23036	127	-22909
ENSMUSG00000027996	Sfrp2	Sfrp2	20319	15	0.1612	1.682	23080	187	-22893
ENSMUSG00000034981	Parm1	Parm1	231440	16	0.3366	1.653	23072	203	-22869
ENSMUSG00000030268	Bcat1	Bcat1	12035	17	0.4936	1.683	23029	186	-22843
ENSMUSG00000037161	Mgarp	Mgarp	67749	18	0.5997	1.896	22921	109	-22812
ENSMUSG00000024538	Ppic	Ppic	19038	19	0.5538	1.705	22978	175	-22803
ENSMUSG00000053279	Aldh1a1	Aldh1a1	11668	20	0.5043	1.631	23009	214	-22795
ENSMUSG00000052353	9930013L23Rik	9930013L23Rik	80982	21	0.4998	1.568	23026	280	-22746
ENSMUSG00000029581	Fscn1	Fscn1	14086	22	0.6613	2.007	22803	81	-22722
ENSMUSG00000031626	Sorbs2	Sorbs2	234214	23	0.4136	1.49	23054	356	-22698
ENSMUSG00000043091	Tuba1c	Tuba1c	22146	24	0.6018	1.604	22917	230	-22687
ENSMUSG00000038168	Leprel1	Leprel1	210530	25	0.516	1.503	23003	338	-22665
ENSMUSG00000033491	Prss35	Prss35	244954	26	0.3128	1.438	23075	452	-22623
ENSMUSG00000032372	Plscr2	Plscr2	18828	27	0.6036	1.557	22914	295	-22619
ENSMUSG00000000184	Ccnd2	Ccnd2	12444	28	0.6078	1.557	22904	295	-22609
ENSMUSG00000070436	Serpinh1	Serpinh1	12406	29	0.5608	1.462	22970	402	-22568
ENSMUSG00000076934	Iglv1	Iglv1		30	0.6969	1.839	22673	122	-22551
ENSMUSG00000068105	Tnfrsf13c	Tnfrsf13c	72049	31	0.6758	1.63	22763	217	-22546
ENSMUSG00000001131	Timp1	Timp1	21857	32	0.6326	1.503	22871	338	-22533
ENSMUSG00000045128	Rpl18a	Rpl18a	76808	33	0.5471	1.425	22983	478	-22505
ENSMUSG00000003379	Cd79a	Cd79a	12518	34	0.6896	1.647	22711	207	-22504
ENSMUSG00000004814	Ccl24	Ccl24	56221	35	0.6881	1.56	22718	291	-22427
ENSMUSG00000075000	Nrbf2	Nrbf2	641340	36	0.5449	1.385	22985	568	-22417
ENSMUSG00000090710	Gm9513	Gm9513	671003	37	0.7291	1.997	22498	82	-22416
ENSMUSG00000060636	Rpl35a	Rpl35a	57808	38	0.6354	1.44	22855	444	-22411
ENSMUSG00000060636	Rpl35a	Rpl35a	1E+08	38	0.6354	1.44	22855	444	-22411
ENSMUSG00000060636	Rpl35a	Rpl35a	1E+08	38	0.6354	1.44	22855	444	-22411
ENSMUSG00000060636	Rpl35a	Rpl35a	1E+08	38	0.6354	1.44	22855	444	-22411
ENSMUSG00000060636	Rpl35a	Rpl35a	1E+08	38	0.6354	1.44	22855	444	-22411
ENSMUSG00000060636	Rpl35a	Rpl35a	1E+08	38	0.6354	1.44	22855	444	-22411
ENSMUSG00000072918	1700022K14Rik	1700022K14Rik		44	0.7148	1.667	22595	195	-22400
ENSMUSG00000060586	H2-Eb1	H2-Eb1	14969	45	0.6745	1.471	22770	382	-22388
ENSMUSG00000052727	Map1b	Map1b	17755	46	0.4018	1.344	23060	712	-22348
ENSMUSG00000039114	Nm1	Nm1	68404	47	0.4297	1.347	23050	705	-22345
ENSMUSG00000028776	Tinagl1	Tinagl1	94242	48	0.5926	1.371	22935	616	-22319
ENSMUSG00000064865				49	0.4753	1.338	23041	736	-22305
ENSMUSG00000058725	Gm11937	Gm11937	71453	50	0.6872	1.443	22723	432	-22291
ENSMUSG00000058725	Gm11937	Gm11937	1E+08	50	0.6872	1.443	22723	432	-22291
ENSMUSG00000058725	Gm11937	Gm11937	1E+08	50	0.6872	1.443	22723	432	-22291
ENSMUSG00000001865	Cpa3	Cpa3	12873	53	0.2823	1.324	23076	790	-22286
ENSMUSG00000083358	Olfr1004-ps1	Olfr1004-ps1		54	0.6804	1.424	22751	483	-22268
ENSMUSG00000023078	Cxcl13	Cxcl13	55985	55	0.7227	1.563	22542	286	-22256
ENSMUSG00000006205	Htra1	Htra1	56213	56	0.6475	1.37	22834	621	-22213
ENSMUSG00000030770	Parva	Parva	57342	57	0.7184	1.481	22577	370	-22207
ENSMUSG00000020473	Aebp1	Aebp1	11568	58	0.6904	1.416	22703	500	-22203
ENSMUSG00000073412	Lst1	Lst1	16988	59	0.7272	1.522	22507	317	-22190
ENSMUSG00000080992	Psmb5-ps	Psmb5-ps		60	0.7332	1.535	22467	312	-22155
ENSMUSG00000076846	Trav13-2	Trav13-2		60	0.5333	1.314	22992	837	-22155
ENSMUSG00000062433	Krtap6-2	Krtap6-2		62	0.6404	1.34	22848	721	-22127
ENSMUSG00000059852	Kcng2	Kcng2	240444	63	0.7411	1.57	22399	275	-22124
ENSMUSG00000022150	Dab2	Dab2	13132	64	0.7032	1.405	22643	522	-22121
ENSMUSG00000024673	Ms4a1	Ms4a1	12482	65	0.7198	1.434	22567	459	-22108
ENSMUSG00000039956	Mrap	Mrap	77037	66	0.7465	1.568	22356	280	-22076
ENSMUSG00000090838				67	0.6859	1.352	22732	692	-22040
ENSMUSG00000069271				68	0.7709	1.796	22132	136	-21996

Table S3. Differentially expressed genes (≥2.0-absolute-fold-change, P<0.05) following proton activation of OGR1 in murine macrophages. pH 6.7 24 h.

Entrez Gene No.	Symbol/gene	Gene Name
20344	*Selp*	Selectin P (Granule Membrane Protein 140kDa)
13653	*Egr1*	Early Growth Response 1
20299	*Ccl22*	Chemokine (C-C Motif) Ligand 22
12156	*Bmp2*	Bone morphogenetic protein 2
18787	*PAI-1*	Serpine1
57349	*Ppbp*	Pro-platelet basic protein (chemokine (C-X-C motif) ligand 7)
23886	*Gdf15*	Growth Differentiation Factor
14131	*Fcgr3*	Fc receptor, IgG, low affinity III (CD16)
246256	*Fcgr4*	Fc receptor, IgG, low affinity IV (CD16-2)
15370	*Nr4a1*	Nuclear receptor subfamily 4
20343	*Sell*	Selectin, CD62L
54123	*Irf7*	Interferon Regulatory Factor 7
21825	*Thbs1*	Thrombospondin 1
67603	*Dusp6*	Dual Specificity Phosphatase 6
29817	*Igfbp7/8*	Insulin-Like Growth Factor Binding Protein 7
16323	*Inhba*	Activin
20692	*Sparc*	Osteonectin
17228	*Cma1*	Chymase
641340	*Nrbf2*	Nuclear receptor binding factor 2
17227	*Mcpt4*	Mcpt4 mast cell protease 4
20379	*Sfrp4*	Secreted frizzled-related protein 4
14129	*Fcgr1*	Fc Fragment Of IgG, High Affinity Ia, Receptor (CD64)
22339	*Vegfa*	Vascular endothelial growth factor A

REFERENCES

1. Livak KJ, Schmittgen TD. Analysis of Relative Gene Expression Data Using Real-Time Quantitative PCR and the 2−ΔΔCT Method. *Methods.* 2001;25(4):402-408.
2. Xia Y, Schneyer AL. The biology of activin: recent advances in structure, regulation and function. *The Journal of endocrinology.* 2009;202(1):1-12.
3. Escribese MM, Sierra-Filardi E, Nieto C, et al. The prolyl hydroxylase PHD3 identifies proinflammatory macrophages and its expression is regulated by activin A. *J Immunol.* 2012;189(4):1946-1954.
4. Zhang YQ, Resta S, Jung B, Barrett KE, Sarvetnick N. Upregulation of activin signaling in experimental colitis. *American journal of physiology. Gastrointestinal and liver physiology.* 2009;297(4):G768-780.
5. Sierra-Filardi E, Puig-Kroger A, Blanco FJ, et al. Activin A skews macrophage polarization by promoting a proinflammatory phenotype and inhibiting the acquisition of anti-inflammatory macrophage markers. *Blood.* 2011;117(19):5092-5101.